

Final Author Comments

The Arctic Ocean Observation Operator for 6.9 GHz (ARC3O) - Part 1: How to obtain sea-ice brightness temperatures at 6.9 GHz from climate model output

Burgard, C., Notz, D., Pedersen, L.T., Tonboe, R.T.

The Cryosphere, #10.5194/tc-2019-317

RC: Reviewer Comment, **AR: Author Response**, *changed manuscript text*

AR: We thank both reviewers for taking the time to read through our paper with such detailed attention. We acknowledge the concerns about the structure and have focused on restructuring the manuscript more clearly. Also, we are very grateful for all the more localized but precise remarks and suggestions. We hope to have fulfilled your expectations and to have clarified your concerns. Larger changes in the manuscript include:

- A new structure for the discussion of the results, presenting the list of experiments before presenting the results, separated figures for the experiments, and a summarizing table
- Removing the section about snow and atmosphere as they were confusing and not fitting the scope of the study, which is to assess the effect of using simple GCM ice and snow information as input for the brightness temperature simulation

1. Reviewer #1

RC: Reviewer Summary:

The manuscript addresses the simulation of brightness temperature at 6.9 GHz from sea ice (with no consideration of snow cover) using ice property profile (temperature and salinity) resulting from an advanced 1D thermodynamic model and other simplified models. The brightness temperature is simulated using 1D microwave emission model. The main purpose of the study is to examine the sensitivity of the calculated brightness temperature to assumptions of the ice property profiles. With that, the study reached conclusions about the factors that affect the brightness temperature the most, such as the sub-surface salinity of first-year ice and the use of a salinity profile that changes with depth compared to assumption of constant salinity or linear temperature.

With this information, it is possible to develop an observation operator that can be

applied to sea ice simulation by a climate model. While the study offers information towards this purpose it does not actually provide a conclusive answer. Yet, this does not take from the credibility of the study as I see it a pioneering attempt to handle the sensitivity issue using a novel approach of testing the effects of different profile shapes (e.g. constant salinity introduced very large uncertainties in brightness temperature and the two-step linear temperature assumption in snow-covered sea ice does not introduce large uncertainties, etc.).

The manuscript is well written and the subject is timely as the issue of sensitivity of ice parameter estimation (from satellite observations or modeling) has been identified as urgent, a conclusion from a workshop on same subject in Hamburg in October 2017.

I would recommend publication subject to revision that takes into consideration the following comments.

AR: Thank you very much for the positive feedback, and for your detailed, constructive comments on how to further improve our paper. We have addressed all your comments as described in the following.

RC: *Major comments*

First comment: The writing in some parts is confusing. I had to read the same part several times to understand and connect what the authors want to say. Please modify to make the presentation more coherent, especially in the parts that describe the tested profiles (reference and simplified), sections and sub-section titles that do not reflect the contents, etc.

AR: We have tried to clarify the structure, better separating the methods and the results. We also have splitted some of the figures into several figures to make it easier for the reader to follow.

See Sec. 3.4 and Sec. 4

RC: **Second comment: The use of some terminology is confusing such as “water liquid volume fraction”.**

AR: In the process of working on this study, we have moved from using the term "liquid water fraction" to using the term "brine volume fraction". We started with "liquid water fraction" in opposition to "solid ice fraction" but decided to move on with "brine volume fraction" to avoid the confusion you are mentioning. Therefore, there should not have been mentions of "liquid water fraction" left in the manuscript. We apologize for the confusion and have replaced "liquid water" by "brine" in the relevant occurrences.

RC: **Third comment:** Some presented aspects of sea ice physics are not precise. I am suggesting corrections.

AR: Thank you for the suggestions given below. We have taken them into account in the revision of the manuscript.

RC: *Minor comments (All these issues are explained in the following comments. I call it minor though they are many and some may exceed the definition of “minor”.):*

Abstract The last sentence “As periods of melting snow with intermediate moisture content typically last for less than a month,...” needs modification. Snow may become wet during transition seasons (fall and spring) and that leads to anomalous brightness temperature (please see Shokr et al. *Rem Sensing of Env*, 123,(2013), and Ye et al., *IEEE TGRS*, 54(5) (2016)).

AR: We have tried to clarify based on your suggestion as follows:

Finally, in our setup, we cannot assess the effect of wet snow properties. As periods of snow with intermediate moisture content, typically occurring in spring and fall, locally last for less than a month, our approach allows one to estimate realistic brightness temperatures at 6.9 GHz from climate model output for most of the year.

RC: **P3 L9:** suggest using “loss” instead of “permittivity”

AR: We have reformulated this sentence as follows:

It depends on the temperature distribution in the medium and on the transmission and reflection affecting the path of the microwave radiation from the emitting layer within the medium to the surface of the medium.

RC: **P3 L11:** This paragraph is about the emissivity (emitted radiation) from snow-covered sea ice. It needs modifications as I find confusion between using the terms emissivity and permittivity. Here is some information that might be useful in rephrasing the sentences. (1) permittivity determines the reflection/absorption at a surface of dielectric mismatch but emissivity determines the emitted radiation (in TIR or MW bands). (2) While there is relation between the emissivity and reflectivity, there is no relation between emissivity and permittivity. (3) The sentence “This means that water is a stronger absorber than pure ice in the microwave range” is not correct because water has high permittivity as you mentioned in the first sentence, therefore it is high reflector in the MW bands (but not in the TIR). (4) When the snow becomes wet or the ice surface is flooded, the emissivity increases due to the more absorption of solar radiation by water contents (nothing to do with the permittivity). So, to conclude this point, the authors can just focus on the emissivity in this paragraph and remove all connections to the permittivity. Emissivity

and permittivity are used in modeling MW emission when layers are assumed (water/ice/snow/air) but this is not the subject of the paragraph.

AR: We apologize for the confusion due to using "permittivity" instead of "emissivity". Thank you for the clarification. We have restructured this section to clarify that we are describing the radiative properties of the layered snow and ice column, influencing the resulting brightness temperature and therefore the permittivity is important.

See Sec. 2

RC: P3 L16: the sentence “In snow, liquid water is mainly present during melting periods” needs correction. Please see my comment about the Abstract.

AR: We have tried to clarify following your suggestion above. We now write:

If the snow becomes wet, as happens during melting periods and localized events of warm air advection mainly occurring in spring and fall, the dielectric loss in the snow layers increases substantially, leading to a reduction in the transmissivity of the snow layer to microwave radiation.

RC: P3 L21: the opening of this paragraph “The scattering of the microwave radiation in sea ice is a function of...” Once again, the theme here should be the emitted radiation, hence the focus should be placed on the two forms of extinction, the absorption and the scattering. Also, since you include the atmosphere, it is better to mention “the satellite observation of microwave radiation from sea ice” in the first sentence.

AR: Thank you for pointing out that this sentence was not precise. We have restructured Sec. 2 to correct the imprecision.

RC: P3 L26: you can add “air bubbles in MYI” and mention something about the MW wavelength in relation to the typical size of brine pockets, snow grain, air bubbles and atmospheric droplets.

AR: We have added the air bubbles and typical sizes of the scattering bodies into the text. We now write:

In general, scattering affects the brightness temperature measured from space over sea-ice surfaces increasingly with increasing frequency (Tonboe et al., 2006) as the wavelength successively approaches the size of brine pockets and air bubbles on the order of tenths of millimeters to millimeters, snow grains on the order of hundreds of micrometers to millimeters and atmospheric aerosols and droplets on the order of micrometers.

RC: P4 L21 This last sentence in the paragraph is clumsy. Please clarify and simplify.

AR: Thank you for pointing that out. We have reformulated as follows:

This is a necessary first step to understand fundamental drivers of the brightness temperature before comparing brightness temperatures simulated on the basis of MPI-ESM output directly to brightness temperatures measured by satellites, which we do in Burgard et al., 2020.

RC: P4 L13 Make it “our reference profiles”.

AR: Done.

RC: P5 L1-5: Any reason why you did not use ERA5?

AR: Most of the analysis presented here was conducted and finished before the release of ERA5. However, we do not expect the choice of reanalysis data to substantially affect the results of the study in any case, as the analysis focuses on conceptual findings, not tied to the exact timing and location of the forcing.

RC: P5 L11. You provide example to show that simulated sea-ice evolution is not necessarily representative for the real sea-ice evolution at location 75°N, 00°W. You can mention another example at 90°N as this location may not have MYI in all years. Please see maps of MYI in Fig. 8 in Ye et al. (2016) (mentioned above). The maps were generated from a retrieval method using satellite microwave observations.

AR: As mentioned in the manuscript, we do not claim to simulate the sea-ice evolution at the given location and time realistically. This is because SAMSIM always assumes a seasonal cycle for the oceanic heat flux to the bottom of the ice following the oceanic heat flux measured during the SHEBA campaign north of Alaska. Under the combination of ERA-Interim atmospheric forcing and this SHEBA oceanic forcing, sea ice can form at 75N00W and the ice at the North Pole survives the summer melt. This also means that locations which usually have MYI as pointed out in the reference you give might not have MYI in our simulations.

As suggested by reviewer #2, we have tried to explain the principle and location more conceptually. This highlights that the locations for which the ERA-Interim forcing was chosen cannot be compared to these locations in reality. We have included the information about the exact location for reproducibility in the caption of Fig.2. We have reformulated as follows:

We conduct our analysis using atmospheric forcing from two random points in the Arctic Ocean as input for SAMSIM. At the first point, the combined forcing of the ERA-Interim atmospheric variables and the SHEBA oceanic flux leads to complete melting of the simulated ice in summer each year, resulting in several

cycles of first-year ice. At the second point, the combination of the atmospheric forcing and oceanic heat flux leads to a simulated ice cover present throughout the year, resulting in several cycles of multiyear ice (Fig.2). This way, we capture potential differences in the brightness temperature simulation depending on the ice type. To ensure that the conclusions we draw from these two random points are robust, we have conducted the same analysis on five additional random points distributed in the Arctic Ocean and the results support our conclusions.

RC: **P6 Fig.2** the difference between the black and grey lines is not obvious although it is easy to understand what each color indicates. The peak of the ice thickness in June is NOT a “comfortable” result. Equally “uncomfortable” is the rate of MYI thickness increase. My expectation is that MYI thickness increase should take place at a slower rate.

AR: As mentioned in the caption, the peak of ice thickness in June is a model artifact. As they represent only a very small fraction of data points, we do not expect this to have an effect on our results. However, to avoid confusion, we have now masked these points out for the study. Regarding the rate of increase of MYI, we agree with you. In this case, we are looking at a comparably fast growth because it is comparably thin MYI. Compared to the FYI growth rate in the left panel of Fig.2, the MYI growth rate is slower.

RC: **P7 L6:** Do you mean “incoming longwave radiation” instead “microwave radiation”?

AR: We mean microwave radiation. This is the radiation normally referred to as the down-welling microwave radiation. This represents all microwave radiation reaching the ground from the atmosphere. Contributors to this radiation are background space radiation, clouds and water vapour in the atmosphere, and oxygen. However, we set it to 0 K in our setup because we are mainly interested in the effects of sea-ice physical properties on the brightness temperature. We have reformulated as follows:

These are the correlation length, the brine pocket form, the incidence angle, the ocean temperature, the incoming microwave radiation from the atmosphere (i.e. the cosmic background radiation and the radiation reflected and emitted by properties of the atmosphere) and the ice-ocean reflectivity for vertical polarization.

RC: **P7 L7:** Table 1, not Tab. 1

AR: Changed.

RC: **P7 L10:** just to complete the physics picture, you may add the loss and scattering (extinction) caused by snow wetness, brine wicking, and snow metamorphism.

Then you can state that you ignored these effects (the 6.9 GHz is not affected by the grain metamorphism as mentioned before in the text)

AR: We have now separated this explanation into dry and wet snow and added your suggestion as follows:

The effect of wet snow on the brightness temperature is larger and depends on the snow wetness, brine wicking, and snow metamorphism.

RC: P7 L15: it is good to mention this limitation on the application of your study. Just want to remind you, once again, of the possibility of the wet snow during the transition seasons as indicated above.

AR: We have reformulated as follows:

However, when comparing results of a possible observation operator based on this study to actual observations, we strongly recommend to not consider periods of wet snow, during melting periods and events of warm air advection, as setting the snow wetness to zero will lead to unphysical brightness temperatures in these periods.

RC: P7 Table1: did you mention the source of these data? If not please do.

AR: We have now added the sources for these constants in the caption as follows:

MEMLS constant input details and properties of the snow layer. The incidence angle is from AMSR-E and AMSR2, passive microwave sensors measuring at 6.9 GHz (NASDA, 2003; JAXA, 2011). The ocean temperature and snow density are the constant values used in a GCM such as MPI-ESM (Wetzel et al., 2012; Giorgetta et al., 2013). The incoming microwave radiation from the atmosphere is set to 0 K because we want to focus on the effect of sea-ice properties on the emitted radiation. Correlation lengths are based on past experiments conducted by R.T. Tonboe.

RC: P7 last 3 lines (no line numbers in the manuscript): this is the first time you mention “brine pocket form”. I am not familiar with MEMLS but does it need the geometry of brine pocket? This parameter is not mentioned in Table 1.

AR: MEMLS assumes either random needles or spherical pockets. We use the spherical pockets assumption but as scattering is negligible at 6.9 GHz, we argue that the choice of brine pocket form will not affect our results substantially. We have added the information about the brine pocket form in Table 1 and added following sentence in the text:

In any case, we assume that the choice of brine pocket form will not affect our result substantially because scattering within the ice is negligible at 6.9 GHz.

RC: The influence of vertical sea ice properties Should this section be called “Results”??

AR: In the course of restructuring the manuscript, we now call this "Results".

RC: P8 second paragraph.... Here are a few observations that might be used to improve the text. First, the salinity profile is always of C-shape as long as the cold temperature prevails. There is a physical explanation. It changes when the temperature rises in the spring. You can refer to the book of Weeks (2015) “On Sea Ice” or the book you already quoted by Shokr and Sinha. Second, the shape of brine pockets does not depend on age but, as rightly stated, on the initial formation process of sea ice. The assumption of spherical pockets may be valid for frazil ice. This is common in the subsurface layer of Antarctic ice and it exists in the Arctic when ice is formed under turbulent oceanic conditions.

AR: Thank you, this is useful information. We have reformulated following your input: *The salinity parametrization used in Sec. 4.2.2 is based on an "L-shape" of the salinity profile, while the sea-ice salinity profile often resembles a "C-shape" or even a "T-shape" when cold temperatures prevail (Nakawo and Sinha, 1981; Shokr and Sinha, 2015a).*

and:

However, it is known that the brine pocket form highly depends on the initial formation process of the ice, which is not simulated.

RC: P8 Section 4 and section 4.1. The titles do not reflect the contents. For example, Section 4 “The influence of vertical sea ice properties” include Fig. 3, which is about effect of sub-surface salinity (not vertical profile). Also, Section 4.1 “Brine volume fraction” has information about the temperature profile at the end. Please re-organize the information to make improve the flow of the information.

AR: Thank you for your input. We have taken this comment into account when we restructured the manuscript. We have now called the Section containing Fig.3 "Subsurface properties vs. Vertical profile".

RC: P8 in Section 4.1, the authors kept mentioning “ice surface brine volume” while they mean sub-surface. Please replace “surface” with “sub-surface” and define the subsurface depth, at least roughly.

AR: We apologize for the confusion. In this case our subsurface is the upper 1 centimeter. We now follow your suggestion by using the term "ice subsurface brine volume".

RC: **P9 L1:** the sentence “Especially above an ice surface brine volume fraction of 0.2,...” is awkward. You may say “when ice surface brine volume fraction is higher than 0.2 ...”. Also, it is not right to say “brightness temperature at the ice surface”. Just say “brightness temperature from the ice cover”. Then, in the following sentence you can say that the radiation is mainly coming from the surface.

AR: Thank you for the suggestion. We have now changed the sentence as follows:
When the ice subsurface brine volume fraction is higher than 0.2, the brightness temperature from the ice column is linearly related to the ice subsurface brine volume fraction (Fig. 3, bottom row).

RC: **P9 L4:** in the sentence “brightness temperature transitions roughly linearly ..” you may change the word “transitions” to “varies”.

AR: Done.

RC: **P9 L8:** the sentence “In our SAMSIM profiles, these high surface brine volume fractions fractions occur predominantly in summer, i.e. from April to September” is correct although the word “fractions” is repeated. I would like to draw the authors’ attention to an estimation of brine volume fraction which we performed (experimentally) on Arctic sea ice and found that the fraction in the sub-surface layer (top 5 cm) exceeds 0.2 only when the average temperature exceeds -3°C. It is possible that the temperature of this layer reaches this value in the beginning of the freezing season. But this note does not affect the work in your study.

AR: Thank you for pointing this repetition out. We think that your observations are in line with our findings. Thanks for sharing these! We have added this information by completing the following sentence with "the beginning of the freezing season":
In our SAMSIM profiles, these high subsurface brine volume fractions occur predominantly in warm conditions, i.e. from April to September, during the melting period and in the beginning of the freezing season.

RC: **P9:** Figure 3 and the conclusions from this figure are interesting.

AR: We agree, thank you.

RC: **P9** last paragraph (no line number)... you talk about “surface liquid water fraction” and “ice surface brine volume fraction”. It is a bit confusing. On P8 L28 you mention “liquid water in the form of brine”, which is a bit ambiguous. Brine is brine! And the dissolved salt (not water) is the material that causes loss of MW signal. I would suggest avoiding liquid water and just keep “brine”. The liquid water fraction is relevant only to the snow at the onset of melt. Related to this

point, you mentioned "For surface liquid water fractions below 0.2, occurring in both winter and summer..." But Fig.3 shows surface brine volume fraction, NOT liquid fraction. Also, you said "For these low ice surface brine volume fractions,...". What are those low fractions? Please fix this issue of liquid water versus brine volume fraction. It is only brine. Not liquid water.

AR: Again, we apologize for the confusion. As mentioned in an answer to a previous comment, in the process of working on this study, we have moved from using the term "liquid water fraction" to using the term "brine volume fraction". We started with "liquid water fraction" in opposition to "solid ice fraction" but decided to move on with "brine volume fraction" to avoid the confusion you are mentioning. Therefore, there should not have been mentions of "liquid water fraction" left in the manuscript. We apologize for the confusion and have replaced "liquid water" by "brine" in the relevant occurrences.

RC: **P10 L1-5:** it is mentioned that brightness temperature of thin MYI in summer drops to about 180K and that is attributed to the saline layer at the bottom of the ice. It is true that MYI thickens (grows) when winter returns and there is a layer of saline FYI at the bottom. But why do you say the emitted radiation mainly comes from this layer? The entire volume of the ice radiates. And the radiation from the bottom layer may be completely scattered by the bubbles, which concentrate at the to 20 cm or so.

AR: The influence of the bottom salinity on the MYI brightness temperature was inferred from investigating the different input profiles one by one. These low MYI brightness temperatures were found in September, in the first two weeks of the re-freezing period. In the corresponding input profiles, the ice salinity is zero for all layers except in the bottom layer, where new saline ice is forming. As scattering is negligible at 6.9 GHz, the brightness temperature can be influenced by this bottom layer. However, we agree that this might not necessarily be realistic and that the conditions leading to these salinity profiles could be investigated further. As a side note, this phenomenon does not occur anymore when using simplified temperature and salinity profiles. We have reformulated as follows:

In some multiyear ice cases during warm conditions, the brightness temperature drops below 240 K at near-zero subsurface brine volume fractions. These low brightness temperatures occur in September, in the first two or three weeks in which ice growth sets in again. In these cases, the ice column used as input for MEMLS has a brine volume fraction of zero over the whole column, except in the bottom layer. We therefore suggest that the simulated brightness temperature is mainly influenced by the very saline bottom layer at the interface between ice and ocean in these cases, leading to low brightness temperatures. This behaviour is not necessarily realistic and the conditions leading to these input salinity profiles might need further investigation.

RC: **P10 L6** “Unfortunately for the higher brightness temperatures around 260 K at low ice surface brine volume fractions, we could not infer...”. Are you going back to the FYI here? You are in the middle of discussing MYI.

AR: We have now restructured this discussion and hope it is clearer.

RC: **P10 L9:** Again, you mention “liquid water fraction profile”. You probably mean brine fraction. Saline FYI ice has solid ice, brine, air and sometimes solid salt if temperature drops below the precipitation point of the salt. MYI has only solid ice and air. The term liquid water fraction is confusing for me.

AR: Again, we apologize for the confusion. This has been corrected.

RC: **P10 L1:** brightness temperature from MYI is around 180K in winter (low value because of the scattering from air bubbles) and it increases in summer due to surface flooding. That is why you found higher values of 260K. Please correct this information.

AR: This is not the case here. Our high values around 250 K are what is expected at 6.9 GHz. Typical tie-points values for winter MYI lie near 250 K (e.g. Ivanova et al. 2015, TC Vol9(5) use 246K). Low brightness temperatures for MYI are only occurring in our simulation in rare occasions during September in the beginning of the freezing season.

RC: **P10 L10-14:** The information in this paragraph should be combined with information in the first paragraph in section 4.2 (Fig.4). The current text is confusing. What is the simplified profile? Constant for salinity and linear for temperature? Then why do you include a non-linear salinity in Fig. 4 and call it also “simplified”? Also, MPI-ESM uses the constant salinity and temperature profile. True? Is that the reason you tested the effect of constant salinity on brightness temperature? This is the most confusing part for me. Please re-write to make the information more organized and coherent.

AR: Again, this comment has been taken into account for the new structure. We hope it is clearer now.

RC: **P10 L21:** The title of 4.2 does not express the contents. We find data from Reference salinity, Reference temperature and Salinity as function of depth. Also, I would suggest presenting all these options in a table that shows the values, the functions (if any) and the method for each option. That will make it easier for the reader to follow the text and interpret the figure better.

AR: Again, this comment has been taken into account for the new structure. We also have

added Table 2, which includes the information about the experiment setup and the results.

RC: P10 L22: “as would be given...” or better be “as would be used...”?

AR: Replaced.

RC: P12 and P13: in the captions of Fig.5 and Fig.6 you should mention the season of the data (Oct.-March) and (April-Sept.), respectively.

AR: Thank you for pointing that out. We have added this clarification.

RC: P14 L8-9: This is the first time the explanation of the non-linear profile in Fig. 4 is explained. That is what I mean by re-organizing the information. I was wondered about this curve while reading, until I reached the explanation here.

AR: We have re-organized the manuscript so that the two profiles are discussed in the beginning of Sec.4.2.2. We now write the following:

In the experiment SIMPLESALCONST, we explore the effect of a constant salinity profile on the simulated brightness temperature. MPI-ESM assumes a constant salinity of 5 g/kg regardless of sea-ice type or age. As this is clearly too high for multiyear ice (Ulaby et al., 1986), we assume a constant salinity of 5 g/kg for first-year ice and a constant salinity of 1 g/kg for multiyear ice throughout the ice column in our simplified salinity profiles (see dashed lines in Fig.5).

In the parallel experiment SIMPLESALFUNC, we explore an alternative approach to simplify salinity profiles. We use a parametrization representing salinity as a function of depth (Griegwank and Notz, 2015). This parametrization assumes an L-shaped profile, with low salinity near the surface and a rapidly increasing salinity in the lower ice layers (see Fig.5, full lines, and Table B1). This parametrization has been evaluated against observations (Griegwank and Notz, 2015). In both SIMPLESALCONST and SIMPLESALFUNC, we use the reference temperature profiles simulated by SAMSIM.

RC: P14 Section 4.3: This section highlights the contribution from this study. Would be it useful to compile the statistics of absolute difference in one table to help the reader to explore the impact of each assumption at a glance? The numbers in the text should remain. I am not sure if this suggestion is reasonable but the authors might consider it. The results from using salinity as a function of depth in the case of MYI in summer (Fig. 6) is not the best, contrary to the conclusion in P14 L20.

AR: Yes, the salinity as a function of depth, combined with the linear temperature profile, leads to the best result for MYI in warm conditions (10.5 ± 21.7 K compared to 43.0 ± 45.7 K for constant salinity).

We have followed your suggestion and added Table 2 as a summary of the experiment results.

RC: P14 L28: model or module?

AR: We mean "model" here. We do not plan to integrate the emission model as a module into the climate model but rather to apply it on already produced climate model output.

RC: P16 L2: "relationship only depends on the snow thickness". Why depend on snow thickness? You present the decrease of brightness temperature per unit depth (cm)?

AR: We have removed this section as it was diverting from the main message of the paper, which is the properties of the ice column that are needed. Instead we have added the following paragraph in the initial discussion about potential uncertainties in Sec.3.3:
Another limitation in the input data for MEMLS is the snow information. We investigated the indirect effect of the snow cover on the simulated brightness temperature, e.g. the radiative effect (as opposed to the thermal insulation effect), and found that the brightness temperature decreases by approximately 0.13 K for every centimeter of snow present on the ice column. Therefore, although the snow is expected to be "transparent" at less than 10 GHz, lack of information about the snow structure besides snow temperature and thickness might still lead to uncertainties of up to a few K in the presence of a thick snow cover.

RC: P17 L21: "In summer, we cannot reproduce realistic sea-ice surface brightness temperatures due to the very high sensitivity of the liquid water fraction to small changes in salinity near 0°C." Something is wrong here. Brine volume fraction is sensitive to salinity, but liquid water fraction?

AR: Again, we apologize for the confusion. We mean "brine volume fraction" and have replaced it.

RC: P17 L25: the sensitivity of brightness temperature in summer is high because it is related to two parameters which we have no accurate information about; the areal ratio of melt pond and the wetness of the snow or even ice surface as you indicated later. In the next paragraph you mention snow grain as a possible contributor to the brightness temperature in summer. But this influence virtually does not exist at that time.

AR: We agree, this is unclear. We have removed the mention of the influence of snow grains on the brightness temperature in summer.

RC: **P18:** The Outlook section is well composed. It is true that there is lack of comprehensive data on snow property profiles. However, there are many measurements conducted in scattered areas over the past few decades to characterize snow over ice under different atmospheric temperatures. It would be useful if someone compiles this information in one review paper and conclude some gross features that can be used in GCM models.

AR: Yes, we strongly agree that such a compilation of observations would be a very valuable resource for similar studies in the future.

RC: **P18** In the Conclusion section there is no mention about the good use of “salinity as a function of depth”.

AR: We have mentioned the salinity as a function of depth in the point about "cold conditions". We have restructured the conclusion and hope this is highlighted better now. We now write:

Periods of cold conditions

- *Use the temperature profile provided by the GCM if existing. Otherwise, use the simulated snow surface temperature and ocean temperature at the bottom of the ice to infer a two-step linear temperature profile through the snow and ice.*
- *Use the salinity profile provided by the GCM if existing. Otherwise, interpolate the salinity profile as a function of depth, following the functions given by Notz and Griewank, 2015.*
- *Apply an emission model, e.g. MEMLS, to these profiles, combined with information about correlation length, sea-ice type, etc.*
- *Use sea-ice concentration, and atmospheric properties provided by the GCM.*
- *Apply a simple ocean emission model and atmospheric radiative transfer model to account for the influence of open water when the sea-ice concentration is below 100% and for the influence of the atmosphere on the brightness temperature measurements by satellites from space.*

2. Reviewer #2

RC: Reviewer summary:

The authors consider the development of an observation operator to provide passive microwave brightness data at 6.9 GHz frequency and Vertical polarization. The work is motivated by the need to overcome observational uncertainty introduced by geophysical retrieval algorithms applied to satellite observations and used to initialize and evaluate climate models. Here, the observation operator simulates the brightness temperature from the climate model output instead of requiring the retrieved sea ice concentration from observed brightness temperature data. Consideration of the feasibility and limitations of the observation operator concept for simulated sea ice is the main focus here. The authors use highly resolved 1D thermodynamic sea-ice and 1D microwave emission models to consider the effect that the simplified temperature and salinity profiles characteristic of GCM outputs have on brightness temperature estimates and observation operator performance. Generally, the approach works well for cold, winter conditions, and in the peak of summer when surface melt ponds are present, but not during periods of wet snow. The authors determine the boundary conditions for the construction of an operator that is evaluated against satellite brightness temperatures in their companion paper (which I did not evaluate).

In general the paper is well written and the descriptions and figures are mostly clear and concise. Appendix A is useful for providing equations though Appendix B is just a table that could be in the paper. The methods should be better organized, and made to be distinct from the results, to make the paper easier to follow. For example, on Page 10, around line 11, there are new methods and their reasoning described in amongst the section focused on the results presented in Figure 3.

The authors should clarify their positioning on the role that snow plays on the examined 6.9 GHz frequency and vertical polarization, in the contexts of season, ice type, and other available frequencies and polarizations. It is mostly all there, just hard to follow. For example, the negligible contribution of dry snow properties compared to ice (due to brine in the ice) is cited as advantageous for the ≈ 4.3 cm wavelength examined, yet there is a section looking into the role of dry snow (Section 6) and the following statement is made “the radiative effect of the snow cover hence remains important.”. At the beginning of Section 7.3 snow is cited as a limiting factor. Perhaps it is better to make it clearer earlier in the paper that one of the goals of the study is to better understand the potential impact of dry (and wet snow) conditions on the operator output. Statements about wet snow are easier to follow as there are not contradictions.

AR: Thank you very much for the positive feedback, and for your detailed, constructive comments on how to further improve our paper. We have worked on a new structure for the manuscript and have tried to further clarify the issue of snow for our study.

We have addressed your other comments as described in the following.

RC: P3L22: ‘atmosphere’ doesn’t fit here because the sentence is referring to sea ice.

AR: Thank you for pointing that out. We have reformulated the sentence to clarify that we are describing the brightness temperature measured by the satellite from space. We now write as follows:

As brightness temperatures are usually not measured at the ice surface but at the top of the atmosphere by satellites, the microwave radiation emitted by the sea-ice cover can additionally be affected by transmissivity and reflectivity of the snow and atmosphere on the path between the surface and the satellite.

RC: P5L7-10: The purpose behind defining specific locations is unclear. This is especially true since the authors indicate that sea ice seldom exists at the first-year sea ice location. The choice of locations for the sensitivity analysis are also arbitrary. If the choice of location does not affect the study then the locational context isn’t needed.

AR: We have followed your suggestion and now describe the forcing data in a more conceptual way, as follows:

We conduct our analysis using atmospheric forcing from two random points in the Arctic Ocean as input for SAMSIM. At the first point, the combined forcing of the ERA-Interim atmospheric variables and the SHEBA oceanic flux leads to complete melting of the simulated ice in summer each year, resulting in several cycles of first-year ice. At the second point, the combination of the atmospheric forcing and oceanic heat flux leads to a simulated ice cover present throughout the year, resulting in several cycles of multiyear ice (Fig.2). This way, we capture potential differences in the brightness temperature simulation depending on the ice type. To ensure that the conclusions we draw from these two random points are robust, we have conducted the same analysis on five additional random points distributed in the Arctic Ocean and the results support our conclusions.

RC: P7: The paragraph on the bottom, beginning “Our input for the emission model...”, is somewhat dismissive of the breadth of in-situ observations that are available, and the role of these observations in model development. It would be clearer if the authors outlined the model set-up, inputs, and assumptions used, since this is a methods section, and save uncertainty evaluations and suggestions for the discussion section.

AR: We agree that it is more common to discuss uncertainties after presenting the results. However, in this case, we want to make clear to the reader right in the beginning that, while there might be many uncertainties, they do not affect our results substantially.

This way, the reader can concentrate on our results without being concerned about these limitations while reading the paper.

RC: P9L8: Is it correct to say that April in the Arctic is summer?

AR: We apologize for the confusion. To be more precise, we have changed all occurrences of "summer" to "warm conditions" and "winter" to "cold conditions" throughout the manuscript.

RC: P9 Figure 3: Symbols for FYI and MYI are not clear in the figure.

AR: Thank you for pointing that out. We have now divided the results for FYI and MYI in two separate subfigures.

See Fig.3

RC: P14L3: It is confusing that the assumption of constant salinity introduces large uncertainties in the brightness temperature during summer, when earlier the authors mentioned the properties inside the ice do not influence the brightness temperature when the ice surface has a brine volume fraction higher than 0.2 (also during summer). Also on P15 (L7-8) the authors say the brightness temperature depends on the surface rather than internal ice properties. Some clarification given in the context of expected penetration depth would be helpful.

AR: We apologize for the confusion. With a new structure of the manuscript, we hope to have clarified this point. We now use the results of Sec.4.1. to assess in which conditions information about the vertical profile is needed and when not. In many warm conditions cases it is not needed, but there are also warm conditions cases in which the ice subsurface brine volume fraction is below 0.2 and therefore profile information is needed. Also the simplified profiles are also relevant for the subsurface layer (especially for salinity), so this is why we look into the influence of simplified profiles for warm conditions as well.

RC: P16L15-17: Indicate what would happen if ice concentration were <100%.

AR: We have removed this section as it was beyond the scope of this study. We focus on the brightness temperature simulated for a snow and ice column, based on profiles that could be inferred from GCM output. We realize that this section was confusing. Discussing the effect of the atmosphere, which can be accounted for by using a radiative transfer model, and regions of less than 100% sea ice are beyond the scope of this study.

RC: P16L18: Section 7 should be “Discussion and Conclusion”.

AR: We acknowledge that this would be a more typical way of structuring the manuscript.

However, we prefer to keep Section 6 (previously 8) as a short conclusion with the main take-home messages and leave Section 5 (previously 7) to a Summary and Discussion.

RC: P17L19-20: Sentence “In summer...” is confusing i.e. how is the liquid water fraction highly sensitive to changes in salinity. Do you mean the salinity of the melt ponds?

AR: We apologize for the use of "liquid water fraction" here, we actually mean "brine volume fraction". We have replaced it. We mean the salinity of the subsurface layer. The brine volume fraction is highly sensitive to changes in bulk salinity and temperature. As temperatures are near 0°C, ice can only exist at very low salinities. The brine volume fraction increases very fast for low brine salinities (A4) but the salinities we use in our simplified profiles are often of 1 g/kg or even more.

RC: P18L33: The authors should elaborate on how the brightness temperature would be weighted by melt pond fraction.

AR: To weight by melt pond fractions, we suggest using the melt pond fraction given by the GCM and treat it as an open water surface when combining the results of the ocean emission model and our sea-ice brightness temperatures. We have reformulated as follows:

Periods of bare ice near 0 °C

- *Use a constant brightness temperature for the ice surfaces. Burgard et al., 2020 derive a warm conditions sea-ice surface brightness temperature of 266.78 K from observational estimates. This represents a brightness temperature at the top of the atmosphere of 262.29 K corrected by the mean atmospheric effect of 4.49 K in their simulations.*
- *Use sea-ice concentration, melt pond fraction, and atmospheric properties provided by the GCM.*
- *Apply a simple ocean emission model and atmospheric radiative transfer model to account for the influence of open water when the sea-ice concentration is below 100% or when melt ponds are present on the ice and for the influence of the atmosphere on the brightness temperature measurements by satellites from space. If not existing yet, include a routine accounting for the effect of melt ponds additionally to the effect of open ocean surfaces in the surface emission model.*

RC: P19L3: How would periods of wet snow be identified?

AR: We have tried to clarify as follows in the conclusions:
Periods of melting snow

- *Identify periods and locations of reduction in snow thickness at temperatures near 0 °C in the GCM output.*
- *Ignore these points in the analysis. The GCM output does not provide enough information about the snow properties and wet snow strongly affects the brightness temperature.*

RC: **P19 Appendix A: Indicate the validity ranges of the formulas.**

AR: We are sorry if this is not clear. We have added the validity ranges and updated outdated formulas.

See Appendix A

The Arctic Ocean Observation Operator for 6.9 GHz (ARC3O) - Part 1: How to obtain sea-ice brightness temperatures at 6.9 GHz from climate model output

Clara Burgard^{1,2}, Dirk Notz^{1,3}, Leif T. Pedersen⁴, and Rasmus T. Tonboe⁵

¹Max Planck Institute for Meteorology, Hamburg, Germany

²International Max Planck Research School for Earth System Modelling, Hamburg, Germany

³Institute of Oceanography, Center for Earth System Research and Sustainability, Universität Hamburg, Hamburg, Germany

⁴National Space Institute, Technical University of Denmark, Lyngby, Denmark

⁵Danish Meteorological Institute, Copenhagen, Denmark

Correspondence: Clara Burgard (clara.burgard@mpimet.mpg.de)

Abstract. We explore the feasibility of an observation operator producing passive microwave brightness temperatures for sea ice at a frequency of 6.9 GHz. We investigate the influence of simplifying assumptions for the representation of sea-ice vertical properties on the simulation of microwave brightness temperatures. We do so in a one-dimensional setup, using a complex 1D thermodynamic sea-ice model and a 1D microwave emission model. We find that realistic brightness temperatures can

5 be simulated in ~~winter cold conditions~~ from a simplified linear temperature profile and a self-similar salinity profile in the ice. These realistic brightness temperatures can be obtained based on profiles interpolated to as few as five layers. Most of the uncertainty resulting from the simplifications is introduced by the simplification of the salinity profiles. In ~~summer warm conditions~~, the simplified salinity ~~profile leads profiles lead~~ to too high ~~liquid water fractions at the surface~~ ~~brine volume fractions in the subsurface layer~~. To overcome this limitation, we suggest using a constant brightness temperature for the ice
10 during ~~summer warm conditions~~ and to treat melt ponds as water surfaces. Finally, in our setup, we cannot assess the effect of ~~snow properties during melting~~ ~~wet snow properties~~. As periods of ~~melting~~ snow with intermediate moisture content ~~typically typically~~ ~~occurring in spring and fall, locally~~ last for less than a month, our approach allows one to estimate realistic brightness temperatures at 6.9 GHz from climate model output for ~~about 11 months throughout~~ ~~most of~~ the year.

1 Introduction

15 Sea-ice concentration products are retrieved from passive microwave brightness temperatures measured by satellites and come with a non-negligible uncertainty (Ivanova et al., 2015; Tonboe et al., 2016; Lavergne et al., 2019). This observational uncertainty hinders reliable climate model initialization (Bunzel et al., 2016) and model evaluation (Notz et al., 2013). Additionally, it hinders a robust extrapolation of the future sea-ice evolution based on current observations. For example, sea-ice area is strongly coupled to changes in the global-mean air temperature (Gregory et al., 2002; Winton, 2011; Mahlstein and Knutti,
20 2012; Ridley et al., 2012; Li et al., 2013) and thus to CO₂ emissions (Notz and Stroeve, 2016). The relationship between CO₂ emissions, global-mean air temperature and sea ice provides the possibility to project the future Arctic sea-ice evolution

under different forcing scenarios. However, Niederdrenk and Notz (2018) showed that the observational uncertainty in sea-ice concentration translates into uncertainty in the sensitivity of sea ice to changes in global-mean air temperature and therefore leads to uncertainty in the temperature at which an ice-free Arctic in summer can be expected.

Observation operators are a current approach in climate science to circumvent observational uncertainty and the spread 5 introduced by the use of retrieval algorithms on satellite measurements (Flato et al., 2013; Eyring et al., 2019). They simulate directly the observable quantity, in our case the brightness temperature, from the climate model output instead of retrieving the simulated quantity, in our case the sea-ice concentration, from the satellite observations. A sea-ice observation operator reduces the uncertainty introduced by assumptions used in retrieval algorithms about the state of other climatic variables besides the sea-ice concentration. It takes advantage of knowing the consistent climate state in time and space simulated by the climate 10 model alongside the sea ice. This knowledge allows a more comprehensive approach to climate model evaluation, as we cannot only assess the simulated sea-ice concentration but also the simulated sea-ice temperature, snow cover, and sea-ice type. The feasibility and limitations of an observation operator applied to sea ice simulated by a climate model have not been investigated yet. This is the question we address here.

We investigate how important the complexity of the representation of sea-ice properties is for the simulation of sea-ice 15 surface brightness temperatures emitted by different ice types. Experiments using a model accounting for part of the processes at work inside the sea ice combined with an emission model have shown that knowing the vertical sea-ice properties are sufficient to generate realistic microwave brightness temperatures (Tonboe, 2010; Tonboe et al., 2011). We mainly concentrate on the vertical representation of temperature and salinity inside the ice and snow, as they are the main drivers of the liquid brine 20 brine volume fraction in the ice and liquid water fraction in the snow and thus of sea-ice brightness temperatures, especially at low microwave frequencies (Ulaby et al., 1986). As most general circulation models (GCMs) do not explicitly represent the time evolution of vertical profiles of temperature and salinity in the ice and snow, we investigate the effect of simplified temperature and salinity profiles on the simulation of brightness temperatures. We do so by comparing reference profiles, representing an estimate of reality, on the one hand and simplified profiles, representing GCM output, on the other hand in an idealized one-dimensional setup, using a complex thermodynamic sea-ice model and a microwave emission model.

25 We focus on the simulation of sea-ice brightness temperatures at 6.9 GHz at vertical polarization as a first step. At this frequency, the main driver of brightness temperatures are the sea-ice properties, while the contribution of the snow emission and scattering and of the atmospheric absorption and scattering and of the atmosphere due to water vapor, cloud liquid water and temperature are small compared to the surface contribution. The framework can, however, be extended to other frequencies and polarizations in the future, if the increasing importance of the snow and atmospheric contribution with increasing frequency 30 is taken into account.

In Sec. 2, we provide the theoretical background about drivers of sea-ice brightness temperatures and in Sec. 3 we present our method and the sea-ice and emission models used for our experiments. In Sec. ??4, we explore the influence of simplifications in the temperature and salinity profiles on the simulation of sea-ice brightness temperatures to then explore the effect of a reduced number of layers in Sec. ??. To complete the study, we quantify the uncertainty introduced by a snow cover and

the atmosphere in Sec. ??). Finally, we discuss our findings results in Sec. 6 and conclude with suggestions for a functional observation operator for sea ice in Sec. 6.

2 Theoretical background

The brightness temperature TB is a measure for the microwave radiation emitted by one medium or a combination of media and represents corresponds to the temperature of a blackbody emitting the observed amount of radiation. It is defined as:

$$\text{TB} = \epsilon_{\text{eff}} \cdot T_{\text{eff}}$$

where ϵ_{eff} is the emissivity of the emitting part of the medium, i.e. the layers influencing the resulting radiation emitted at the surface and T_{eff} the integrated temperature over this same emitting part (Hallikainen and Winebrenner, 1992; Shokr and Sinha, 2015b; Tonboe et al., 2006). The thickness of the emitting part and its emissivity depends on the temperature distribution in the medium and on the transmission and reflection affecting the path of the microwave radiation from the emitting layer within the medium to the surface of the medium. The transmission and reflection in turn depend on the permittivity and scattering properties of the medium, which in turn depend on the medium and on the frequency and polarization of the radiation.

In the case of sea ice, the permittivity is mainly a function of the fraction and distribution of liquid water in the form of brine inside the ice as the permittivity of water is an order of magnitude higher. Transmission and reflection of the microwave radiation within an ice column are driven by the permittivity and the dielectric loss of the different layers of the ice on the one hand and scatterers present in the ice on the other hand. Sea ice is a mixture of liquid brine and pure ice and the permittivity and dielectric loss of liquid brine are orders of magnitude larger than the permittivity and dielectric loss of pure ice (Ulaby et al., 1986; Shokr and Sinha, 2015a). Therefore, the permittivity and dielectric loss inside a sea-ice column are mainly a function of the fraction and distribution of liquid brine in the different layers of the ice. This means that water is a stronger absorber than pure ice in the microwave range. The liquid water fraction in the snow and, looking at a vertical profile of the ice, ice layers with high brine volume fractions have a lower transmissivity and larger reflectivity than ice layers with low brine volume fractions. The vertical distribution of the brine volume fraction in the ice are is a function of temperature and bulk the vertical distribution of temperature and salinity. Brine is present within the ice throughout the its first year. If the ice becomes multiyear ice, most of its brine will have drained out and the brine volume fraction decreases substantially compared to first-year ice. In snow, liquid water is mainly present during melting periods. Also, the lowest layer of the snow can be saline, especially above first-year ice (Barber et al., 1998; Shokr and Sinha, 2015b), enabling the presence of liquid water at the base of the snow. However, our setup does not allow us to investigate saline snow in this study.

The scattering of the microwave radiation in sea ice within an ice column is a function of the permittivity and the size of scatterers inside the ice, snow, and atmosphere. In first-year ice, the main scatterers are brine pockets, while in multiyear ice the main scatterers are air bubbles, as most of the brine will have drained out (Winebrenner et al., 1992; Tonboe et al., 2006; Shokr and Sinha, 2015a). While a dry atmosphere and dry snow cover have a low permittivity, they can still influence scattering for

As brightness temperatures are usually not measured at the ice surface but at the top of the atmosphere by satellites, the microwave radiation emitted by the sea-ice cover can additionally be affected by transmissivity and reflectivity of the snow and atmosphere on the path between the surface and the satellite. For frequencies below 10 GHz, dry snow is practically “transparent” (Hallikainen, 1989) and the atmosphere has a negligible influence. For frequencies higher than 10 GHz, scattering 5 occurs within a dry snowpack (Mätzler, 1987; Barber et al., 1998). In ~~ice, snow, and atmosphere, the scattering becomes increasingly important~~ general, scattering affects the brightness temperature measured from space over sea-ice surfaces increasingly with increasing frequency (Tonboe et al., 2006) as the wavelength successively approaches the size of brine pockets ~~and air bubbles on the order of tenths of millimeters to millimeters~~, snow grains ~~on the order of hundreds of micrometers to millimeters~~ and atmospheric aerosols and droplets ~~on the order of micrometers~~.

10 If the snow becomes wet, as happens during melting periods and localized events of warm air advection mainly occurring in spring and fall, the dielectric loss in the snow layers increases substantially, leading to a reduction in the transmissivity of the snow layer to microwave radiation. This may also happen when brine wicking takes place in the lowest layer of the snow, especially above first-year ice (Barber et al., 1998; Shokr and Sinha, 2015b). However, we will not attempt to investigate in detail the effect of wet snow on the radiation in this study as our model setup does not allow us to simulate detailed processes 15 within the snowpack.

Sea-ice concentration retrievals are based on satellite measurements at frequencies ranging from 1.4 GHz to 91 GHz (Ivanova et al., 2014, 2015; Gabarro et al., 2017). In the following, we concentrate on radiation at 6.9 GHz and vertical polarization. This frequency is advantageous as, with a wavelength of approx. 4.3 cm, it is only slightly affected by scattering inside the ice, the snow, and the atmosphere. The brightness temperature at 6.9 GHz therefore mainly depends on the ~~emission and absorption~~ 20 ~~properties~~ properties affecting permittivity and dielectric loss of the different layers inside the ice ~~rather than on the scattering properties~~. This is why our focus lies on the properties of the sea-ice column, rather than on the snow structure or the state of the atmosphere. The ~~emitting part of the ice can be~~ penetration depth in ice at 6.9 GHz is around 20 cm ~~thick~~ for first-year ice and around 50 cm ~~thick~~ for multiyear ice (Tonboe et al., 2006). Therefore, we investigate not only the properties of the 25 ice surface but also the properties of the whole sea-ice column to be sure to capture the main influences on the brightness temperature.

3 ~~Method~~ Methods and Data

3.1 ~~Method~~

Although a few GCMs use detailed sea-ice modules (Vancoppenolle et al., 2009; Bailey et al., 2018), most GCMs use very simple sea-ice models that do not resolve the properties driving ~~absorption and scattering~~ microwave transmission and reflection 30 inside the ice and snow. ~~The~~ Ideally, our observation operator would compute brightness temperatures from such a GCM as well. However, it is not clear yet how these simplifications affect a brightness temperature simulated based on a simple representation of the relevant properties.

As a basis to investigate the effect of using non-detailed sea-ice information, we assume that our input for the operator would be output by the Max Planck Institute Earth System Model (MPI-ESM, Wetzel et al., 2012) is such a GCM. In MPI-ESM, sea ice is represented as flat sea ice, with very simple sea-ice properties: a sea-ice (bare ice) or snow (snow-covered ice) surface temperature, a constant sea-ice bottom temperature at -1.8 °C, and a constant salinity of 5 g/kg regardless of sea-ice type or 5 age (Notz et al., 2013). It is not clear yet how these simplifications affect a brightness temperature simulated based on these properties.

To explore the importance of the vertical distribution of sea-ice properties on the simulation of brightness temperatures, we use an idealized one-dimensional setup. This one-dimensional setup works as follows. On the one hand, we use a one-dimensional thermodynamic sea-ice model to simulate our reference profiles (see Sec. 3.1). It computes highly resolved vertical 10 sea-ice profiles under a given atmospheric forcing. On the other hand, we simplify these reference profiles to emulate profiles that could be inferred from information given by MPI-ESM for the same conditions. These two sets of profiles can be used to simulate two sets of brightness temperatures with a microwave emission model (see Sec. 3.2). The two sets of resulting brightness temperatures can then be used to quantify the effect of the GCM simplification on the brightness temperature simulation, compared to our reference (see Fig. 1, Sec. 3.3 and Sec. 3.4).

15 In this setup, we can quantify the influence of each parameter separately on the simulated brightness temperature. We could have compared brightness This a necessary first step to understand fundamental drivers of the brightness temperature before comparing brightness temperatures simulated on the basis of MPI-ESM output directly to brightness temperatures measured by satellites. However, we would then have not been able to infer the contribution to the difference in brightness temperatures of fundamental differences between model and observations on the one hand, and the contribution of the differences in the 20 resolution of the ice properties on the other hand, which we do in Burgard et al. (2020).

3.1 SAMSIM

Our reference profiles are simulated by the 1D Semi-Adaptive Multi-phase Sea-Ice Model (SAMSIM, Griewank and Notz, 2013, 2015). This is a complex thermodynamical model simulating the evolution of a 1D sea-ice column under given surface forcing. It computes sea-ice temperature, salinity, and brine volume fraction profiles on a semi-adaptive grid, with a number 25 of layers varying between 0 and 100. It includes most of the processes governing sea-ice growth and melt, and interactions between the ice and, if existent, its snow cover. It was developed to investigate the brine dynamics inside the ice. A detailed description of underlying equations and represented processes can be found in Griewank and Notz (2013) and Griewank and Notz (2015).

We force SAMSIM with 2 m air temperature, surface downward longwave radiation, surface downward shortwave radiation, 30 and precipitation from the ERA-Interim reanalysis (Dee et al., 2011) in the time period from July 2005 to December 2009. This gives us insight into 4.5 annual cycles, so that we can assess the interannual variability of the growth and melt of sea ice and the evolution of its properties. The ocean salinity is kept at 34 g/kg and the oceanic heat flux at the bottom of the ice is derived from SHEBA measurements, varying between 0 W/m² in spring and 14 W/m² in autumn (Huwald et al., 2005; Griewank and Notz, 2015).

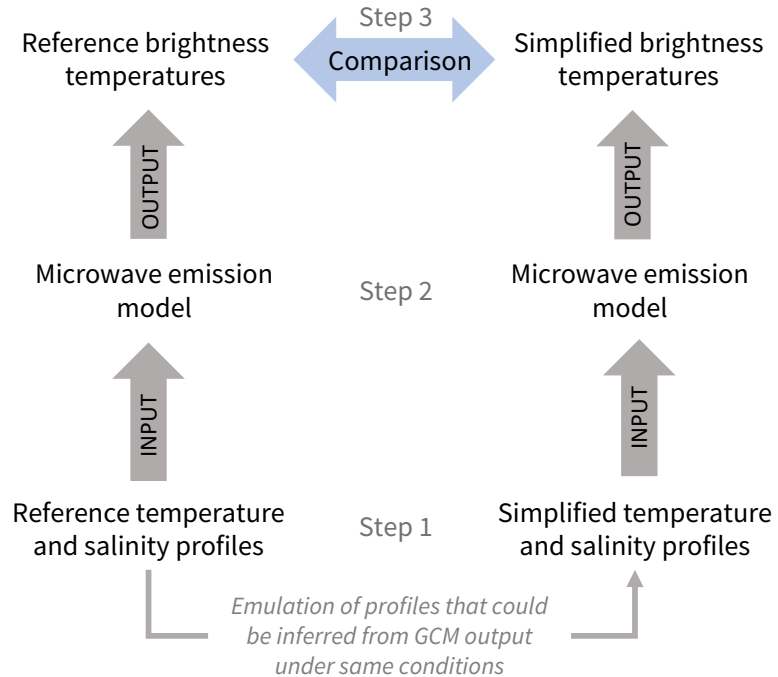


Figure 1. Schematic of the steps of our simulation and comparison method.

To gain insight into differences in microwave emission between first-year ice and multiyear ice, we focus on two. We conduct our analysis using atmospheric forcing from two random points in the Arctic Ocean (Fig. 2). The first point represents as input for SAMSIM. At the first point, the combined forcing of the ERA-Interim atmospheric variables and the SHEBA oceanic flux leads to complete melting of the simulated ice in summer each year, resulting in several cycles of first-year ice at 75°N00°W, 5 where the ice always melts completely in summer. The second point is at 90°N, where the ice survives the melt season and becomes multiyear ice from the second simulation year onwards. Note that in our setup the simulated sea-ice evolution is not necessarily representative for the real sea-ice evolution at that location. For example, sea ice seldom exists at 75°N00°W in reality. The presence of ice in this idealized simulation is likely linked to the oceanic heat flux used. This oceanic flux was measured in the SHEBA site north of Alaska and is very different than in the North Atlantic. However, this does not affect 10 our study because we work in an idealized setup. Also, to ensure our results ice. At the second point, the combination of the atmospheric forcing and oceanic heat flux leads to a simulated ice cover present throughout the year, resulting in several cycles of multiyear ice (Fig. 2). This way, we capture potential differences in the brightness temperature simulation depending on the ice type. To ensure that the conclusions we draw from these two random points are robust, we have conducted the same analysis on five other additional random points distributed in the Arctic Ocean (74°N170°E, 77°N39°E, 80°N160°W, 15 82°N120°W, 85°N50°W) and the results support our conclusions.

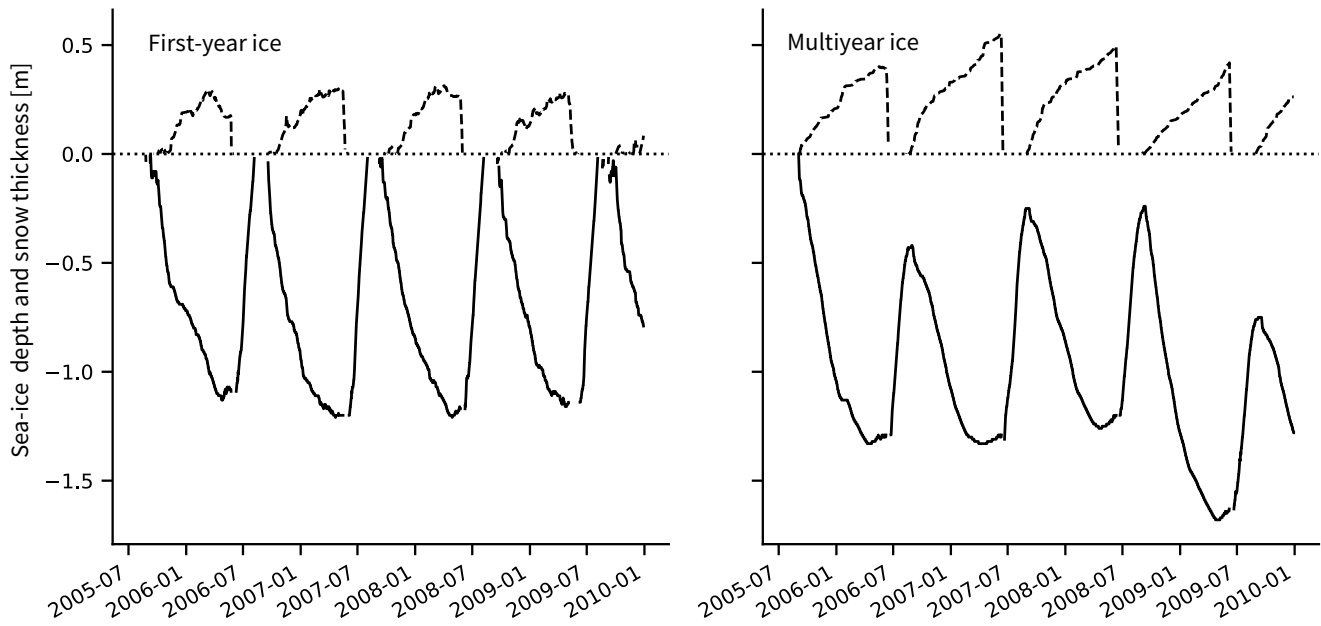


Figure 2. Evolution of sea-ice (black solid line) and snow (grey dashed line) thickness as simulated by SAMSIM under ERA-Interim forcing between July 2005 and December 2009. The peaks—We use ERA-Interim forcing from $75^{\circ}\text{N}00^{\circ}\text{W}$ for the first-year ice and from 90°N for multiyear ice. Note that, to avoid unrealistic model artifacts in the ice thickness during, we have masked out the snow-melt period are a model artifact few timesteps following the final phase of SAMSIM, where snow melt occurs in the form melting of snow-to-slush conversion the snow cover. Also note that the same analysis was conducted using atmospheric forcing from the points $74^{\circ}\text{N}170^{\circ}\text{E}$, briefly increasing $77^{\circ}\text{N}39^{\circ}\text{E}$, $80^{\circ}\text{N}160^{\circ}\text{W}$, $82^{\circ}\text{N}120^{\circ}\text{W}$, $85^{\circ}\text{N}50^{\circ}\text{W}$ (not shown) to ensure the thickness robustness of the top ice layer our results.

3.2 MEMLS

The simulation of sea-ice brightness temperatures is conducted with a slightly modified version of the Microwave Emission Model for Layered Snowpacks (MEMLS) extended to sea ice (Tonboe et al., 2006). MEMLS was first developed by Wiesmann and Mätzler (1999) to simulate brightness temperatures emitted by a snowpack composed of several layers and was later 5 extended to sea ice (Tonboe et al., 2006). MEMLS uses the information of the properties of the ice and snow layers to simulate the path of microwave radiation from the bottom to the surface of the ice and, if present, snow. It uses the thickness, the temperature, the salinity, the density, the correlation length (measure for the scatterer size), the wetness, the brine pocket form, and information about the type of medium (snow, first-year/multiyear ice) of the different sea-ice and snow layers to compute absorption and scattering transmission and reflection of the radiation along the path. This then results in a brightness 10 temperature emitted at the surface of the ice or snow.

Unless otherwise mentioned, we do not take into account the atmosphere in our analysis as its effect is relatively small at 6.9 GHz. The use of the term "brightness temperatures" in the following is therefore equivalent to the use of "brightness temperatures emitted at the surface of the ice and snow column".

3.3 General simulation setup

5 The temperature and salinity profiles produced by SAMSIM are used as input for MEMLS for the simulation of brightness temperatures. Additionally, density profiles are derived from ~~these properties~~ ~~temperature and salinity~~ using relationships given by Notz (2005) (see [App. A](#) [Eq. A5](#)). Next to the temperature, salinity and density profiles, other variables, which are not computed by SAMSIM, have to be provided to MEMLS. These are the correlation length, the ~~brine pocket form, the~~ incidence angle, the ocean temperature, the incoming microwave radiation from the atmosphere ~~and the (i.e. the cosmic background~~
10 ~~radiation and the radiation reflected and emitted by properties of the atmosphere) and the~~ ice-ocean reflectivity for vertical polarization. They are set to constants, listed in [Tab. Table 1](#).

Additionally, except for snow thickness and temperature, snow properties are neither resolved in SAMSIM nor in MPI-ESM. The main effect of snow on the radiation is its ~~Although a dry snow cover is practically "transparent" at frequencies lower than 10 GHz (Hallikainen, 1989), we still need to account for its presence due to one indirect and one direct effect on the brightness temperature. On the one hand, the snow cover leads to the~~ thermal insulation of the ice column and ~~its refractive effect on the radiation induced by the~~ therefore affects the temperature profile inside the ice, which in turn affects the brightness temperature. On the other hand, the difference in density between ice ~~and~~, snow and atmosphere leads to refraction of the radiation at the interface between ice and snow and between snow and atmosphere. The former ~~effect~~ is taken into account through the use of the SAMSIM snow thickness and snow temperature evolution, and the latter is taken into account through the snow thickness and by using a low density ~~of for~~ snow compared to ice. We therefore set all snow properties, except the snow temperature and snow thickness, to constants, also listed in Tab. 1. [In theory](#),

The effect of wet snow on the brightness temperature ~~simulation is affected by~~ is larger and depends on the snow wetness if it is above zero. Neither, ~~brine wicking, and snow metamorphism. As neither~~ SAMSIM or MPI-ESM resolve ~~the liquid water fraction~~ ~~these properties~~ in the snow. ~~In this study, we therefore~~, we set the snow wetness to zero ~~in this idealized study~~.
25 However, ~~in when comparing results of~~ a possible observation operator based on ~~the results from this study~~ ~~this study to actual observations~~, we strongly recommend to not consider periods of ~~melting snow as we do not have the necessary information to simulate plausible brightness temperatures~~ wet snow, during melting periods and events of warm air advection, as setting the snow wetness to zero will lead to unplausible brightness temperatures in these periods.

Our input for the emission model, e.g. salinity, correlation length, brine pocket form, comes with uncertainties. These are 30 mainly caused by a partial or complete lack of in-situ observations ~~of these small-scale properties~~ and the resulting low understanding of their evolution. We therefore recommend more observations of the ice properties, ~~ideally~~ combined with concurrent microwave radiation measurements. A few of such observations exist already, from both laboratory setting and in-situ, but they mainly focus on frequencies higher than 6.9 GHz (e.g. Grenfell et al., 1998; Jezek et al., 1998; Perovich et al., 1998; Hwang et al., 2007). With more combined observations at lower frequencies, we expect that the uncertainty in the brightness tempera-

Table 1. MEMLS constant input details and properties of the snow layer. The incidence angle is from AMSR-E and AMSR2, passive microwave sensors measuring at 6.9 GHz (NASDA, 2003; JAXA, 2011). The ocean temperature and snow density are the constant values used in a GCM such as MPI-ESM (Wetzel et al., 2012; Giorgetta et al., 2013). The incoming microwave radiation from the atmosphere is set to 0 K because we want to focus on the effect of sea-ice properties on the emitted radiation. Correlation lengths are based on past experiments conducted by R.T. Tonboe.

Incidence angle	55°
Ocean temperature	-1.8 °C
Incoming microwave radiation from the atmosphere	0 K
Ice-ocean reflectivity for V-polarization	0.25
<u>Brine pocket form</u>	<u>spherical</u>
Correlation length first-year ice	0.35 mm for depth < 20 cm, 0.25 mm for depth > 20 cm
Correlation length multiyear ice	1.5 mm
Snow thickness	as computed by SAMSIM
Snow density	300 kg/m ³
Snow correlation length	0.15 mm
Snow salinity	0 g/kg
Snow temperature	as computed by SAMSIM

ture simulation can be reduced in the future through further research and better understanding of the components introducing the uncertainty.

For example, a better understanding of the sea-ice salinity evolution would be of advantage. The salinity parametrization used in Sec. 22.4.2.2 is based on an "L-shape" of the salinity profile, while it is argued that the sea-ice salinity profile often 5 resembles a "C-shape" or even a "T-shape" when cold temperatures prevail (Nakawo and Sinha, 1981; Shokr and Sinha, 2015a). Another parameter of uncertainty is the correlation length. Although it is a variable quite well understood and quantifiable for snow (Mätzler, 2002; Proksch et al., 2015; Lemmetyinen et al., 2018), its quantification in sea ice is not clear and its values not well known. On a similar note, MEMLS ~~makes uses~~ assumptions about the form of the brine pockets. In our study we assumed Here, we assume spherical brine pockets. However, it is known that the ~~shape depends highly on the ice age and formation. An extensive summary of the brine pocket form highly depends on the initial formation process of the ice, which is not simulated. In any case, we assume that the choice of~~ brine pocket form ~~can be found in Light et al. (2003)~~ will not affect our result substantially because scattering within the ice is negligible at 6.9 GHz.

Another limitation in the input data for MEMLS is the snow information. We investigated the indirect effect of the snow cover on the simulated brightness temperature, e.g. the radiative effect (as opposed to the thermal insulation effect), and found that the brightness temperature decreases by approximately 0.13 K for every centimeter of snow present on the ice column.

Therefore, although the snow is expected to be "transparent" at less than 10 GHz, lack of information about the snow structure besides snow temperature and thickness might still lead to uncertainties of up to a few K in the presence of a thick snow cover.

Finally, the use of MEMLS as a sea-ice emission model is a source of uncertainty as well. Here again, the lack of measurements of the parameters needed for the brightness temperature simulation and of microwave radiation itself has inhibited 5 a comprehensive evaluation of the sea-ice version of MEMLS simulations against reality. Still, it is accepted as one of the main tools for sea-ice brightness temperature simulations and has shown its strength in several previous studies (Tonboe, 2010; Tonboe et al., 2011; Willmes et al., 2014; Lee et al., 2017).

~~These uncertainties, however, However, the uncertainties listed above~~ only have a limited impact on the present study. We concentrate on a relative comparison, where we change temperature and salinity in the ice to understand their impact on 10 the brightness temperature, but assumptions about ~~correlation length and the snow and ice correlation length~~, the form of brine pockets, ~~and the snow density~~ are the same in our reference and our simplified brightness temperature simulations. The uncertainties will therefore not impact the difference between the two sets of brightness temperatures. Additionally, in regard to the absolute values, ~~?Burgard et al. (2020)~~ show that realistic brightness temperatures can be simulated by MEMLS using 15 the above mentioned uncertain assumptions with slight tuning. The effect of the uncertainties therefore remains small when considering large scales.

3.4 Experiments

The aim of this study is to assess if realistic brightness temperatures can be simulated for 6.9 GHz, vertical polarization, using 20 the limited information about sea-ice properties provided by a GCM such as MPI-ESM. This assessment is conducted through a range of experiments. In a first step (see Sec. 4.1), we investigate the influence of the ice surface and subsurface properties on the radiation emitted by the snow-ice column. We examine in which conditions information about the vertical profile is needed for realistic brightness temperatures to be simulated and in which conditions information about surface and subsurface properties is enough.

In a second step (see Sec. 4.2), we examine the effect of assuming a linear temperature profile and of different assumptions 25 for the simplification of the salinity profile on the simulated brightness temperature. In this set of experiments, we compare brightness temperatures simulated based on SAMSIM profiles (in the following our *reference profiles*) and brightness temperatures simulated based on the *simplified profiles*. The simplified input profiles are interpolated to the same number of layers as the reference profiles (ranging from 1 to 100 layers, depending on the ice thickness).

In a third step (see Sec. 4.1), we examine the effect of reducing the vertical resolution on the simulated brightness temperature. To do so, we interpolate the vertical properties on fewer layers than the reference profiles.

4 The influence of vertical sea-ice properties

4.1 Subsurface properties vs. Vertical profile

4.2 Brine volume fraction

Sea-ice brightness temperatures at 6.9 GHz are mainly driven by the distribution of liquid water in the form of brine inside the

5 ice, as absorption plays the permittivity and dielectric loss of the ice layers play a larger role than scattering at this frequency.

We compute the ice surface brine volume fraction with Eq. A4 based on the ice surface temperature and salinity profiles given by SAMSIM and find that this relationship is clearly visible in the brightness temperatures simulated based on the vertical profiles from SAMSIM output. The brightness temperatures show a strong dependence on the ice surface. Comparing the ice

10 subsurface brine volume fraction, i.e. in the top ice layer (upper one centimeter) of the profiles, with the simulated reference

brightness temperatures, the relationship between brine volume fraction and brightness temperature is clearly visible. The

brightness temperatures show a strong dependence on the ice subsurface brine volume fraction (Fig. 3a, top row).

If we concentrate the brightness temperature simulation on the ice layers, i.e. using only the properties of the ice layers of the snow and ice column as input to MEMLS, the slight offset in the brightness temperature introduced by the refraction due to

the snow cover is removed and the relationship is even clearer (Fig. 3b, bottom row).

15 Especially above an ice surface When the ice subsurface brine volume fraction of is higher than 0.2, the brightness tem-

perature at the ice surface from the ice column is linearly related to the ice surface subsurface brine volume fraction (Fig. 3b,

bottom row). This means that no radiation signal from below the surface subsurface layer influences the brightness temperature

but only the surface and only the brine volume fraction in the upper centimeters of ice matters. The brightness temperature

transitions varies roughly linearly between brightness temperatures typical for ice (≈ 260 K) at an ice surface subsurface brine

20 volume fraction of 0.2 and brightness temperatures typical for open water (≈ 160 K) at an ice surface subsurface brine volume

fraction of 1. The properties inside the ice do therefore not influence the brightness temperature when the ice surface has a brine

volume fraction higher than 0.2. In our SAMSIM profiles, these high surface subsurface brine volume fractions fractions occur

predominantly in summer warm conditions, i.e. from April to September, during the melting period and in the beginning of the

freezing season. We therefore suggest that an ice surface subsurface brine volume fraction above 0.2 can be interpreted both as

25 very wet ice or as a measure for the melt-pond fraction. This strong relationship means that, when the brine volume fraction

is above 0.2, the subsurface properties play the main role for the brightness temperature simulation and vertical properties are

not necessarily needed.

For surface liquid water fractions below 0.2, occurring in both winter and summer, the spread between brightness temperatures

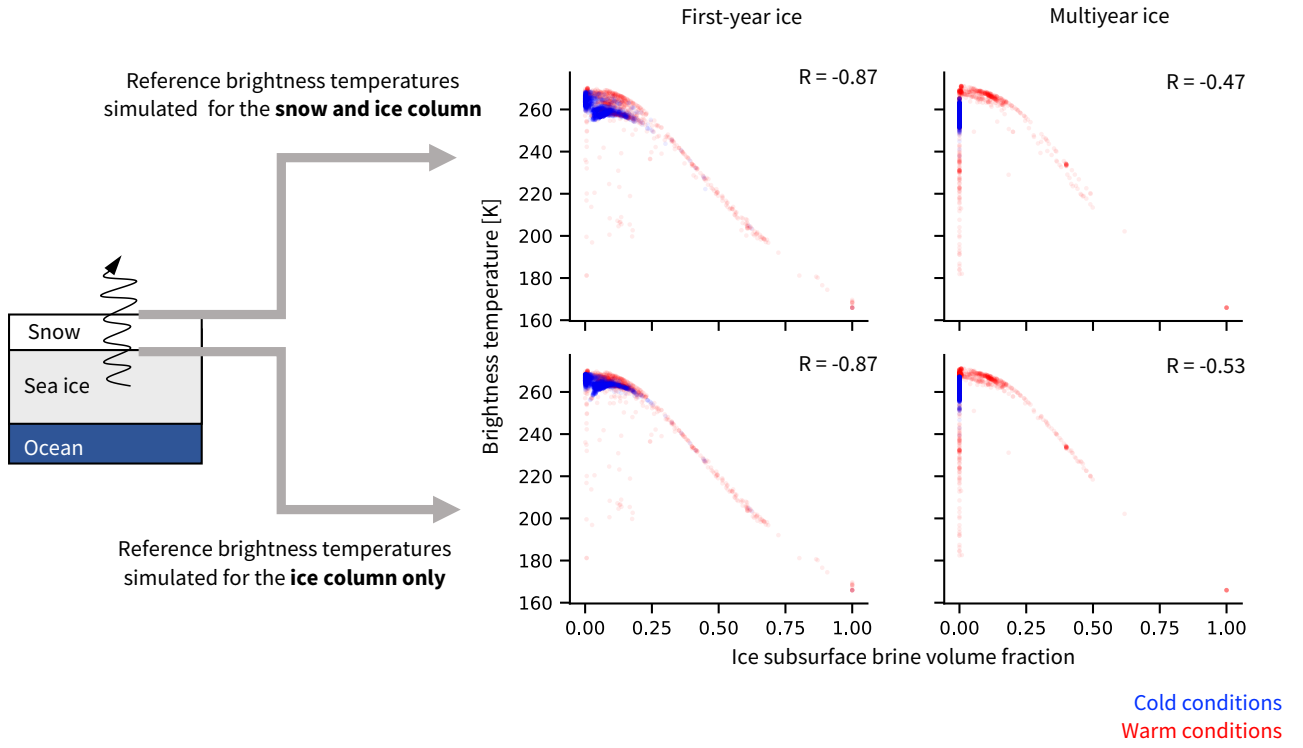
is 10 to 15 K for similar ice surface brine volume fractions. For these low ice surface brine volume fractions, the brightness

30 temperatures are driven by the distribution of brine further inside the ice, which is a function of the temperature and salinity

distribution. In some summer

In some multiyear ice cases during warm conditions, the brightness temperature drops to ≈ 180 K below 240 K at near-zero

subsurface brine volume fractions. These low brightness temperatures occur in September when thin multiyear ice is entering



Reference brightness temperatures at 6.9 GHz, vertical polarization, simulated based on the (a) ice and snow column and on the (b) ice column only as a function of the reference ice surface brine volume fraction. Circles represent first-year ice (FYI), crosses represent multiyear ice (MYI). Blue is winter (October to March), red is summer (April to September). R is the correlation coefficient between the brightness temperature and the ice surface brine volume fraction for both ice types.

Figure 3. Reference brightness temperatures at 6.9 GHz, vertical polarization, simulated based on properties simulated by SAMSIM for the ice and snow column (top row) and on the ice column only (bottom row) as a function of the reference ice subsurface brine volume fraction for first year-ice (left column) and multiyear ice (right column). Blue is cold conditions (October to March), red is warm conditions (April to September). R is the correlation coefficient between the brightness temperature and the ice subsurface brine volume fraction.

the freezing period. Then, the simulated ice column, in the first two or three weeks in which ice growth sets in again. In these cases, the ice column used as input for MEMLS has a brine volume fraction of zero over the whole column, except in the bottom layer. The radiation is therefore We therefore suggest that the simulated brightness temperature is mainly influenced by the very saline bottom layer at the interface between ice and ocean in these cases, leading to low brightness temperatures.

5 **Unfortunately for the higher brightness temperatures** This behaviour is not necessarily realistic and the conditions leading to these input salinity profiles might need further investigation.

Otherwise, for subsurface brine volume fractions below 0.2, occurring in both cold and warm conditions, the brightness temperatures vary by 10 to 15 K around 260 K for similar ice subsurface brine volume fractions. For these low ice subsurface

brine volume fractions, the brightness temperatures are driven by the distribution of brine further inside the ice, which is a function of the temperature and salinity distribution. Unfortunately, for these brightness temperatures around 260 K at low ice surface subsurface brine volume fractions, we could not infer a direct relationship between the brightness temperature and a given layer or a given brine volume fraction inside the ice from our data. We therefore proceed with sensitivity experiments 5 to investigate the effect of simplifications in This implies that information about the vertical distribution of temperature and salinity profiles, and therefore in liquid water fraction profiles, on the simulated brightness temperature, and consequently brine volume fraction, throughout the ice column is necessary to simulate realistic brightness temperatures.

These sensitivity experiments demonstrate what happens when information about the vertical sea-ice profile lacks, as in the sea-ice representation by MPI-ESM. To this end, we compare brightness temperatures simulated based on SAMSIM profiles 10 (in the following our reference) and brightness temperatures simulated based on simplified profiles (in the following our simplification). Our focus is on the influence of the ice properties on the brightness temperature. We therefore only use the ice layers of the ice and snow column as input for MEMLS. This way, the thermal insulation effect of the snow on the temperature profiles is conserved but the refraction at the ice-to-snow interface is neglected for the moment. This treatment corresponds to assuming that the snow is transparent to microwave radiation at this frequency. The refraction effect of the snow is discussed 15 in Sec. ???. From this first look at the relationship between ice properties and simulated brightness temperatures, we conclude that information about the vertical profiles of brine volume fraction are necessary for the simulation of brightness temperatures for cold conditions and for parts of the warm conditions. The effect of describing the brine volume fraction profiles through simplified temperature and salinity profiles on the brightness temperature simulation is what we investigate in a next step.

The purpose of the sensitivity experiments is to identify the influence of the different profiles rather than the effect of 20 differences in the vertical resolution, i. e. the number of ice layers. The simplified input profiles are therefore interpolated to the same number of layers as

4.2 Simplifying the temperature and salinity profile

The brightness temperature emitted by a snow and ice column is mainly driven by the distribution of the brine volume fraction 25 in the ice column. As the brine volume fraction can be described as a function of temperature and salinity, we now investigate the effect of reduced information availability about these profiles, as would be the case in GCM output, on the reference profiles (ranging from 1 to 100 layers, depending on the ice thickness) simulated brightness temperatures.

4.3 Linear Temperature and Constant Salinity

In a first experiment, we investigate

4.2.1 Simplifying the temperature profile

30 We start by investigating the brightness temperature simulated based on information as would be given by a temperature profile as could be inferred from MPI-ESM . For the simplified temperature profile, output. We call this experiment SIMPLETEMP.

MPI-ESM computes a sea-ice (bare ice) or snow (snow-covered ice) surface temperature and a constant sea-ice bottom temperature at -1.8°C . Therefore, we suggest using a two-step linear profile, we through snow and ice. We use the snow surface temperature as simulated by SAMSIM and infer the ice temperature at the interface between ice and snow from it, following Eq. A6. From this ice surface temperature, we interpolate the temperature profile linearly to the ice bottom layer, which has a temperature of -1.8°C . For the salinity profile,

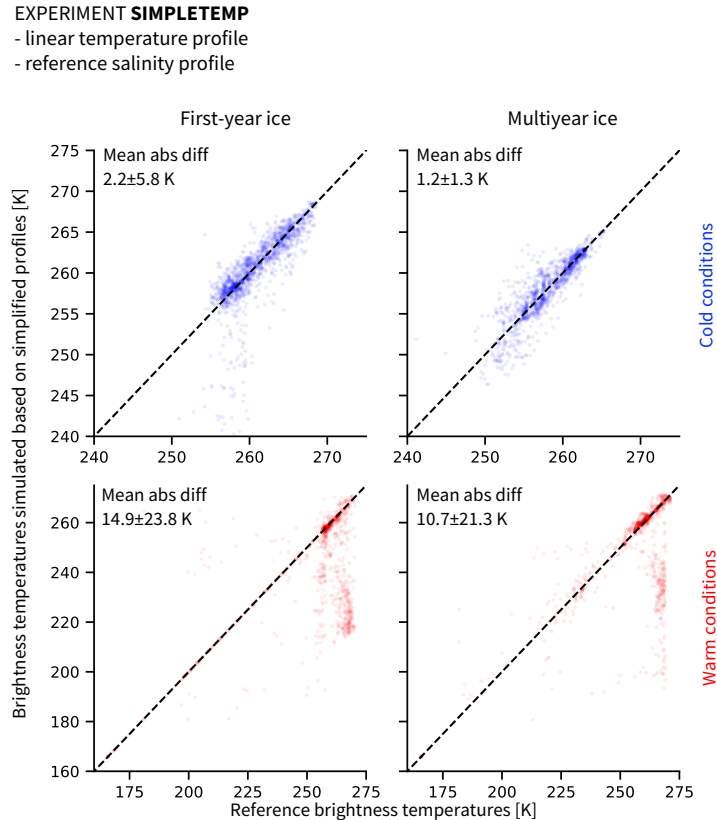


Figure 4. Brightness temperatures at 6.9 GHz, vertical polarization, simulated based on linear temperature profiles and reference salinity profiles (experiment SIMPLETEMP) as a function of reference brightness temperatures. Left column: first-year ice, right column: multiyear ice. Top row: Cold conditions (October to March), bottom row: Warm conditions (April to September). Note that the axes for cold conditions are limited to the range between 240 to 275 K for clarity. The remaining brightness temperatures are scattered between 165 and 240 K and represent around 2% of the simplified data and 0.4% of the reference data.

The influence of the simplifications is clearly different depending on the season. We therefore divide our results into cold conditions (October to March, see Fig. 4, top row) and warm conditions (April to September, see Fig. 4, bottom row). In cold conditions, the absolute difference between brightness temperatures simulated from simplified profiles and brightness temperatures simulated from reference profiles remains small for both first-year ice ($2.2 \pm 5.8 \text{ K}$) and multiyear ice ($1.2 \pm 1.3 \text{ K}$).

In warm conditions, this absolute difference increases by approximately one order of magnitude to 14.9 ± 23.8 K (first-year ice) and 10.7 ± 21.3 K (multiyear ice). The assumption of a two-step linear temperature profile in the snow and ice does therefore not introduce large uncertainties in the brightness temperature simulation in cold conditions but should be used with care in warm conditions.

5 4.2.2 Simplifying the salinity profile

In the experiment SIMPLESALCONST, we explore the effect of a constant salinity profile on the simulated brightness temperature. MPI-ESM assumes a constant salinity of 5 g/kg regardless of sea-ice type or age. As this is clearly too high for multiyear ice (Ulaby et al., 1986), we assume a constant salinity of 5 g/kg for first-year ice and a constant salinity of 1 g/kg for multiyear ice throughout the ice column in our simplified salinity profiles (see dashed lines in Fig. 5).

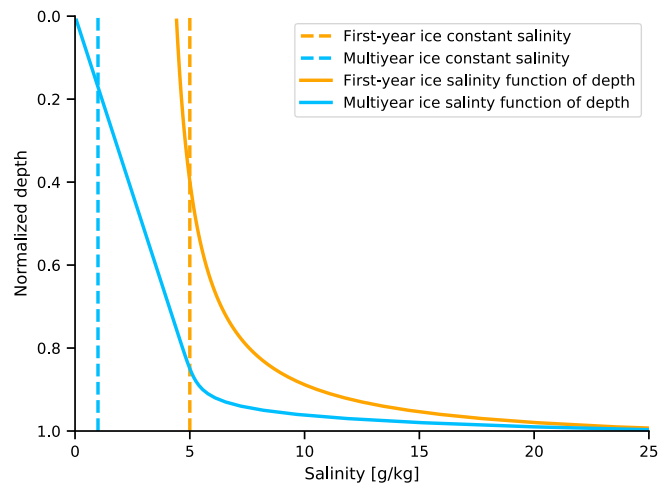


Figure 5. Salinity profiles used for the simplified profiles in Sec. FYI: First-year ice, MYI: Multiyear ice 4.2.2. The dashed lines represent the constant salinity profiles used in Sec. ?? and the full lines represent the salinity profiles as a function of depth used in Sec. ?? The colours represent the different ice types.

10 The influence of the simplifications is clearly different. In the parallel experiment SIMPLESALFUNC, we explore an alternative approach to simplify salinity profiles. We use a parametrization representing salinity as a function of depth (Griewank and Notz, ??). This parametrization assumes an L-shaped profile, with low salinity near the surface and a rapidly increasing salinity in the lower ice layers (see Fig. 5, full lines, and Table B1). This parametrization has been evaluated against observations (Griewank and Notz, 2015). In both SIMPLESALCONST and SIMPLESALFUNC, we use the reference temperature profiles simulated by SAMSIM.

15 Again, we divide the results depending on the season. We therefore divide our results into winter (October to March, see While, for first-year in cold conditions, the effect of using a constant salinity (SIMPLESALCONST) is as low as using a linear temperature profile, with an absolute difference between the brightness temperatures based on simplified profiles and

a) EXPERIMENT SIMPLESALCONST

- reference temperature profile
- constant salinity profile

b) EXPERIMENT SIMPLESALFUNC

- reference temperature profile
- salinity profile as a function of depth

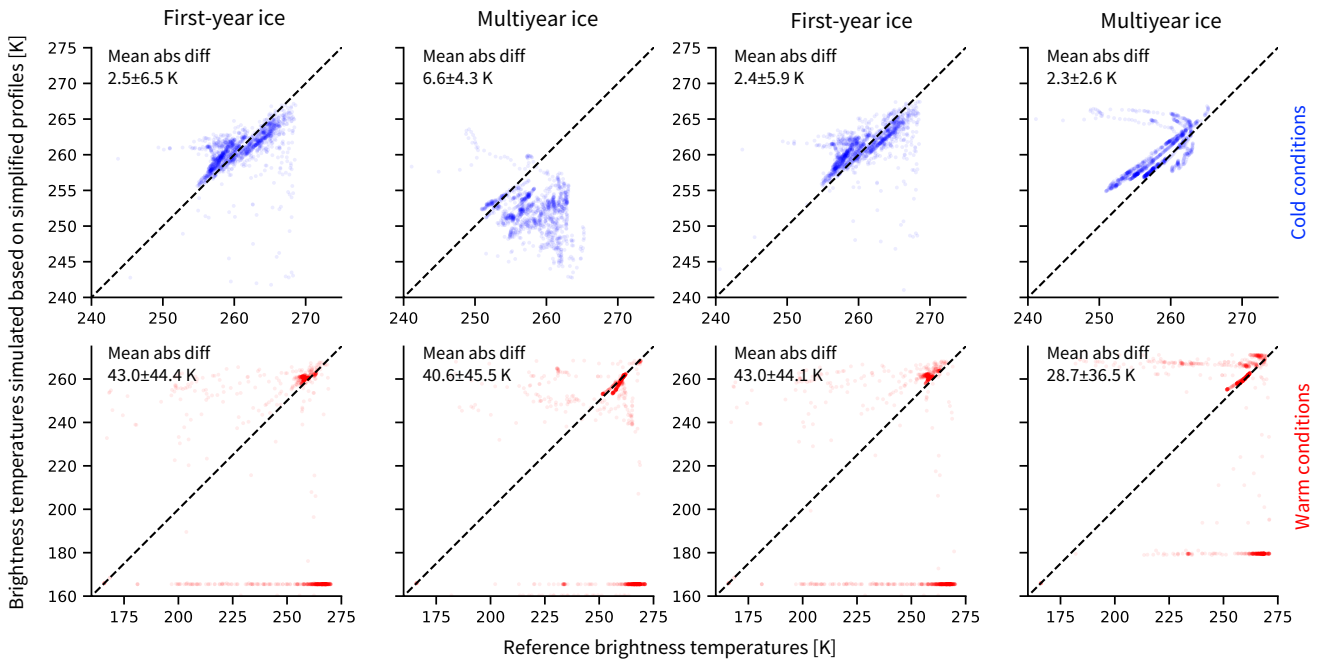


Figure 6. Brightness temperatures at 6.9 GHz, vertical polarization, simulated based on reference temperature profiles and (a) constant salinity profiles (experiment SIMPLESALCONST) or (b) salinity profiles as a function of depth (experiment SIMPLESALFUNC) as a function of reference brightness temperatures. 1st and 3rd column: first-year ice, 2nd and 4th column column: multiyear ice. Upper row: Cold conditions (October to March), lower row: Warm conditions (April to September). Note that the axes for cold conditions are limited to the range between 240 to 275 K for clarity. The remaining brightness temperatures are scattered between 165 and 240 K and represent around 2% of the simplified data and 0.4% of the reference data.

the reference brightness temperature of 2.5 ± 6.5 K, the absolute difference reaches 6.6 ± 4.3 K for multiyear ice (Fig. ??) and summer (April to September, see 6a, top row). In warm conditions, the mean absolute differences are one order of magnitude higher, 43.0 ± 44.4 K for first-year ice and 40.6 ± 45.5 K for multiyear ice (Fig. 6a, bottom row).

If the brightness temperature is simulated based on reference temperature profiles and on the salinity profiles as a function of depth (SIMPLESALFUNC, Fig. ??). In winter, the simplified profiles produce 6b), the uncertainty is similar to the uncertainty introduced by using a constant salinity profile for first-year ice (2.4 ± 5.9 K in cold conditions and 43.0 ± 44.1 K in warm conditions). However, for multiyear ice, the uncertainty introduced by using salinity profiles as a function of depth is lower than the uncertainty introduced by assuming that the salinity is constant throughout depth (2.3 ± 2.6 K in cold conditions and

28.7 ± 36.5 K in warm conditions). We therefore recommend using an ice salinity profile as a function of depth rather than a constant salinity profile as a simplification.

4.2.3 Combining simplified temperature and salinity profiles

In the experiments SIMPLETEMP, SIMPLESALCONST and SIMPLESALFUNC, we learned about the individual effects of using simple temperature and salinity profiles on the brightness temperature simulation. To confirm the conclusion that using both a linear temperature profile and a salinity profile as a function of depth will lead to realistic brightness temperatures, we conduct two additional experiments, combining our simplifications. In the experiment SIMPLEALLCONST, we combine linear temperature profile and constant salinity profile. In the experiment SIMPLEALLFUNC, we combine linear temperature profile and salinity profile as a function of depth.

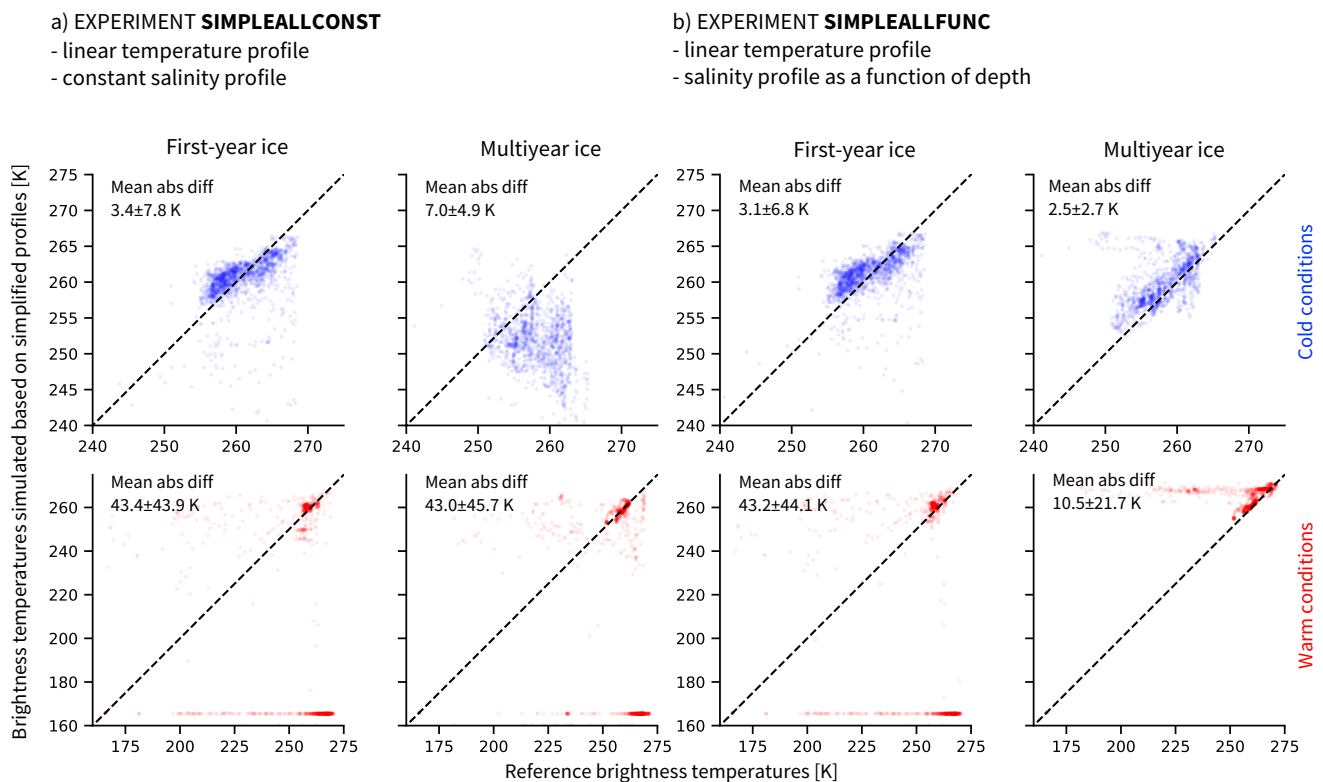


Figure 7. Brightness temperatures at 6.9 GHz, vertical polarization, simulated based on two-step linear temperature profiles and (a) constant salinity profiles (experiment SIMPLEALLCONST) or (b) salinity profiles as a function of depth (experiment SIMPLEALLFUNC) as a function of reference brightness temperatures. 1st and 3rd column: first-year ice, 2nd and 4th column column: multiyear ice. Top row: Cold conditions (October to March), bottom row: Warm conditions (April to September). Note that the axes for cold conditions are limited to the range between 240 to 275 K for clarity. The remaining brightness temperatures are scattered between 165 and 240 K and represent around 2% of the simplified data and 0.4% of the reference data.

The results confirm the findings from the previous experiments. In cold conditions, the combination of simplified temperature and salinity profiles leads to brightness temperatures close to reference brightness temperatures for first-year ice, with a mean absolute difference of 3.2 K the set of profiles using the salinity as a function of depth introducing slightly less uncertainty (3.1 ± 7.6 K) than the set using constant salinity (3.4 ± 7.8 K) (Fig. 22, first row, 1st and 3rd column). For multiyear ice, the spread is higher and there is a tendency of simplified brightness temperatures to underestimate the mean absolute difference between the brightness temperatures simulated based on the simplifications and the reference brightness temperatures, with a mean absolute difference of 7.2 K is clearly lower when using profiles with a salinity as function of depth (2.5 ± 5.0 K) than when using constant salinity profiles (7.0 ± 4.9 K).

Brightness temperatures at 6.9 GHz, vertical polarization, simulated based on different simplified profiles as a function of reference brightness temperatures for winter. Left column: first-year ice, right column: multiyear ice. Note that the axes are limited to the range between 240 to 270 K for clarity. The remaining brightness temperatures are scattered between 165 and 240 K and represent around 2% of the simplified data and 0.4% of the reference data.

Brightness temperatures at 6.9 GHz, vertical polarization, simulated based on different simplified profiles as a function of reference brightness temperatures for summer. Left column: first-year ice, right column: multiyear ice.

In summer, the In warm conditions, mean absolute differences are one order of magnitude higher, with 43.21 ± 43.94 K for than in cold conditions, and similar for first-year ice and 43.02 ice with both salinity assumptions (43.4 ± 45.73 K for multiyear ice (43.9 K using constant salinity and 43.0 ± 44.1 K using salinity as a function of depth). For multiyear ice, again, the uncertainty is clearly lower when using profiles with a salinity as function of depth (10.5 ± 21.7 K) than when using constant salinity profiles (43.0 ± 45.7 K) (Fig. 22, first row). Simplified and reference brightness temperatures are clearly different most of the time. 7, 2nd and 4th column). Reference brightness temperatures and brightness temperatures simulated based on simplified profiles remain clearly different in warm conditions.

Especially, the simplified brightness temperature brightness temperature based on simplified profiles is close or equal to 160 K, i.e. open water brightness temperatures, at most of the time steps in warm conditions. This is because in summer, in warm conditions, the physical temperature of the ice surface approaches 0 °C and, the closer it gets to 0 °C, the lower the salinity must be in order for dry ice to exist rather than slush. At high temperatures and salinities of 5 above 0 g/kg, the brine volume (both salinity simplifications for first-year ice, constant salinity for multiyear ice, see Fig. 5), the subsurface brine volume fraction therefore approaches 1 very fast, leading to low brightness temperatures. For multiyear ice, the effect of a salinity of 1 g/kg on the ice surface brine volume fraction is visible in a similar way. At subsurface brine volume fractions near 1, the brightness temperatures approaches the brightness temperature of open water, as shown in Sec. 4.1.

To confirm our findings for summer and understand further our findings for winter, we conduct two additional sensitivity experiments. In the first experiment, the simplified brightness temperature is simulated based on the linear temperature profiles and the reference salinity profiles. In the second experiment, on the contrary, the simplified brightness temperature is simulated based on the reference temperature profiles and the constant salinity profiles. This enables us to separate the effect of the two simplifications. In both seasons, the effect of the constant salinity assumption is the main driver of the spread between the

different brightness temperatures (Fig. ?? and Fig. ??, third row), while the linear temperature assumption has a small effect on the spread in winter and summer brightness temperatures (Fig. ?? and Fig. ??, second row).

Table 2. Summary of the results of the experiments investigating the effect of simplifying temperature and salinity profiles on the brightness temperature simulation. See Sec. 4.2 for more information.

We therefore conclude that the assumption of a two-step linear temperature profile in the snow and ice does not introduce large uncertainties in the brightness temperature simulation. The assumption of constant salinity, however, introduces very large uncertainties in summer and smaller but still non-negligible uncertainties for multiyear ice in winter. We therefore explore another simplification approach for salinity profiles in a next step.

4.3 Linear Temperature and Salinity as a function of depth

An alternative approach to simplify salinity profiles is a parametrization representing salinity as a function of depth (Griewank and Notz, 2015). This parametrization assumes an L-shaped profile, with low salinity near the surface and a rapidly increasing salinity in the lower ice layers (see Fig. 5, full lines, and Tab. B1).

We now simulate the brightness temperature based on the linear temperature profiles and on the salinity profiles as a function of depth (Fig. ?? and Fig. ??, fourth row). With a mean absolute difference of

Experiment	
<u>SIMPLETEMP</u>	
<u>SIMPLESALCONST</u>	
<u>SIMPLESALFUNC</u>	
<u>SIMPLEALLCONST</u>	
<u>SIMPLEALLFUNC</u>	function of depth (Fig. ?? and Fig. ??, fifth row), it becomes clear that the assumption in the salinity profiles is the main

Through these experiments, we investigated the effect of the simplification of temperature and salinity profiles on the simulated brightness temperature. A summary of the setup and results of the different experiments can be found in Table 2. As a conclusion, we recommend using a two-step linear temperature profile in snow and ice and an ice salinity profile as a function of depth when simulating brightness temperatures based on GCM output –for cold conditions. For warmer and wet 5 subsurface conditions, we recommend exploring possibilities to describe surface and subsurface properties as good as possible because the ice subsurface brine volume fraction is the main driver of the simulated brightness temperature.

The effect of temperature and salinity distribution being clearer now, we turn to another characteristic of GCMs, the limited vertical resolution owing to computational efficiency. Indeed, computing vertical temperature and salinity profiles based on the 10 surface temperature and sea-ice thickness given by a GCM adds a vertical dimension to a two-dimensional output. This means that the computation time and power needed by an operator applied to a GCM will be much higher than a one-dimensional setup. We therefore investigate the importance of the vertical resolution in a next step.

5 The influence of vertical spatial resolution

4.1 Reducing the vertical resolution

Applying an emission model to a GCM consumes high computation power, as the input profiles must be prepared and the 15 emission model ~~must~~ ~~would have to~~ be applied to many grid cells. In the case of the Arctic Ocean at the MPI-ESM low atmospheric resolution of 1.9° , this would mean for example ≈ 4000 data points per timestep. As ocean components in GCMs often have higher horizontal resolution than the atmosphere, this would mean even more computation power needed when using oceanic variables. Reducing the number of layers for the brightness temperature simulation is a possible aspect to reduce the computation time. This is the issue we explore in the following.

20 The simplified profiles used for sensitivity experiments in Sec. ?? 4.2 are interpolated to the same number of layers as the reference profiles, i.e. a variable number of layers depending on the ice thickness between one and 100 layers. We now run the brightness temperature simulation with the ~~simplified profiles (linear temperature, recommended simplified profile, i.e. linear temperature and~~ salinity as a function of depth~~),~~ interpolated on ten, seven, five, and three equidistant layers and compare the results to the reference brightness temperatures. We also include the ~~experiment of Sec. ?? as~~ brightness temperatures from the 25 ~~experiment SIMPLEALLFUNC, which is interpolated to the same number of layers as the reference profiles, as~~ an indicator for the minimal simplified uncertainty in the comparison. We concentrate on ~~winter months~~ cold conditions (October to March), as we showed that the uncertainty in ~~summer~~ warm conditions is already very large at high vertical resolution and mainly depends directly on the ~~surface~~ upper centimeters rather than on properties further inside the ice.

We find that the difference in uncertainty remains small between the reference simplification between 1 and 100 layers and 30 the interpolation on ten, seven, or five layers, the mean uncertainty varying between 2.9 and 3.1 K for first-year ice and between 2.4 and 2.5 K for multiyear ice (see Tab. 3). Using three layers, the uncertainty increases slightly by 0.4 K for the former and by 0.8 K for the latter but still remains small. We therefore argue that using as few as five ~~layers~~ is as reasonable as ~~using~~ 100 layers for the simulation of simplified brightness temperatures.

Table 3. Absolute mean difference and standard deviation [K] between simplified brightness temperatures simulated based on profiles interpolated on different number of layers and reference brightness temperatures simulated based on profiles covering 1 to 100 layers, depending on the thickness of the ice. These values only represent [winter cold conditions](#) (October to March).

	3 layers	5 layers	7 layers	10 layers	1 to 100 layers
First-year ice	3.3±6.9	3.1±6.8	3.1±6.8	3.1±6.8	2.9±6.6
Multiyear ice	3.3±2.7	2.4±2.7	2.4±2.7	2.4±2.7	2.5±2.6

5 The influence of snow [Summary](#) and [atmospheric](#) [discussion](#)

Until now, we concentrated on the influence of sea-ice properties on the simulation of brightness temperatures emitted at the surface of the ice. These simulations included the thermal insulation effect of the snow but did not take into account the refraction effect of the snow cover on the radiation and the path of the radiation through the atmosphere. These are assumed to be small at 6.9 GHz. Nevertheless, it is of interest to quickly investigate the radiative effect of snow cover and atmosphere on the brightness temperature for uncertainty quantification and attribution.

We include the radiative effect of the snow cover in the brightness temperature simulation by using both snow and ice layers of the reference input profiles as input for [MEMLS](#). Except thickness and temperature, which are computed by [SAMSIM](#), all other variables are set to constants (Tab. 1), as neither [SAMSIM](#) nor [MPI-ESM](#) compute more details about the snow properties.

Especially, we only consider dry snow in this study.

The main driver for the radiative effect of the dry snow cover is its density difference to the ice and atmosphere and its thickness. The density difference, and therefore the permittivity difference, between snow and ice on the one hand and between snow and atmosphere on the other hand leads to refraction of the radiation at its boundaries. The snow thickness also has an influence. A linear regression between snow thickness and differences between the simulated brightness temperatures with and without snow layer in winter gives a decrease by 0.13 K (0.13 K for first-year ice, 0.14 K for multiyear ice) for each cm of snow and an intercept of around -1.5 K (-1.7 K for first-year ice, -1.4 K for multiyear ice). This relationship only depends on the snow thickness and the density difference between snow and ice and between snow and atmosphere. It is independent of the snow temperature in our setup. In winter, using both ice and snow layers of the profile leads to a mean effect of -2.7 ± 2.1 K for first-year ice and -3.8 ± 2.4 K for multiyear ice on the brightness temperature compared to only using the ice layers of the profile. Although scattering is limited, the radiative effect of the snow cover hence remains important.

We consider only dry snow here as we do not know anything about the vertical profiles inside the snow from neither [MPI-ESM](#) nor [SAMSIM](#). As liquid water and its distribution within the snow strongly affects the brightness temperature, we do not yet have a reliable solution to simulate the sea-ice brightness temperature when covered by wet snow.

We investigate the influence of the atmosphere with a similar approach as the influence of the snow cover. A simple atmospheric radiative transfer model developed by [Wentz and Meissner \(2000\)](#) is applied using the brightness temperatures simulated based on the reference ice and snow input profiles as the lower boundary conditions. The atmospheric effect mainly depends on the columnar liquid and water vapor content, which we again take from the [ERA-Interim](#) reanalysis, and on oxygen

absorption, included in the radiative transfer model. Assuming a sea-ice concentration of 100%, the absolute mean impact of the atmosphere on the total brightness temperature is between 0.1 and 0.3 K between October and March, between 0.1 and 2 K between April and September.

6 Summary and Discussion

5 5.1 Brightness temperatures for cold conditions

5.2 Winter brightness temperatures

We showed that in winter, we We showed that in cold conditions (October to March), we can reproduce realistic sea-ice surface brightness temperatures using a two-step linear temperature profile in ice and snow and an ice salinity as a function of depth as input for an emission model. The remaining uncertainty is mainly driven by the simplification of the sea-ice salinity distribution. These realistic brightness temperatures can be reproduced with similar uncertainty using as few as five layers. A very high vertical resolution of the ice properties is therefore not needed. The refraction induced by the snow cover affects the brightness temperature, depending on its thickness, by 2.7 to 3.8 K. The atmosphere above the ice and snow column is negligible with an effect reaching at most 0.3 K at 100% sea-ice concentration.

This study was motivated by the fact that observational uncertainty could be reduced by the approach of an observational operator. It is however not trivial to evaluate this proposition based on our results. To compare the uncertainty [K] introduced by the brightness temperature simulation to uncertainties [%] introduced by a sea-ice concentration retrieval algorithm, we translate the uncertainty in brightness temperature into uncertainty in sea-ice concentration.

A simple retrieval algorithm to retrieve sea-ice concentration *SIC* is given by

$$20 \quad \text{SIC} = \frac{\text{TB} - \text{TB}_w}{\text{TB}_i - \text{TB}_w}, \quad (1)$$

with TB the total brightness temperature (ice and open water combined), TB_w a typical open water brightness temperature, and TB_i a typical sea-ice brightness temperature. If we introduce uncertainties ΔSIC and ΔTB in the previous equation, this leads to

$$25 \quad \text{SIC} + \Delta\text{SIC} = \frac{\text{TB} + \Delta\text{TB} - \text{TB}_w}{\text{TB}_i - \text{TB}_w}, \quad (2)$$

resulting in

$$25 \quad \Delta\text{SIC} = \frac{\Delta\text{TB}}{\text{TB}_i - \text{TB}_w}. \quad (3)$$

In our simulated reference brightness temperatures, study, we only simulated brightness temperatures of the snow and ice column. To infer an example for TB_i and TB_w from our results, we use our finding from Sec. 4.1 that the simulated brightness temperature for ice with low subsurface brine volume fraction is representative for a dry snow and ice column and the simulated brightness temperature for ice with very high subsurface brine volume fraction is comparable to the brightness temperature

for open water. From these results we can therefore infer a TB_i , here the simulated brightness temperature for ice with low ~~surface~~ ~~subsurface~~ brine volume fraction, ~~varies~~ ~~varying~~ around 263 K (263.8±3.6 K for first-year ice and 263.7±4.3 K for multiyear ice) and a TB_w , here the simulated brightness temperatures at very high ~~surface~~ ~~subsurface~~ brine volume fractions, ~~varies~~ ~~varying~~ around 166 K (166.1±0.7 K for first-year ice and 165.9±0.1 K for multiyear ice). Following Eq. 3, in this 5 range spanning approximately 100 K, an uncertainty of 1 K in brightness temperature therefore approximately translates into 1% of absolute uncertainty in sea-ice concentration. The observational uncertainty of sea-ice concentration in ~~winter~~ ~~cold~~ ~~conditions~~ is up to 2.5% in consolidated ice and up to 12% for marginal ice zones (Ivanova et al., 2015). The uncertainty of the simulated brightness temperatures translates to a similar range. This might, at first glance, not appear as a solution to drastically 10 reduce the observational uncertainty. However, an observational operator is consistent in time and space and therefore allows a process-understanding of the uncertainties in brightness temperature simulations and, in a possible next step, in retrieval algorithms.

5.2 ~~Spring and summer brightness~~ Brightness temperatures for warm conditions

In ~~summer~~ ~~warm~~ ~~conditions~~ (~~April to September~~), we cannot reproduce realistic sea-ice surface brightness temperatures due to the very high sensitivity of the ~~liquid~~ ~~water~~ ~~subsurface~~ brine volume fraction to small changes in salinity near 0 °C. We therefore 15 recommend using another approach to simulate ~~summer~~ ~~brightness~~ ~~temperatures~~ ~~brightness~~ ~~temperatures~~ ~~for~~ ~~warm~~ ~~conditions~~. We suggest assuming that the brightness temperature of ~~summer~~ ~~warm~~ bare ice is similar all over the Arctic, as temperatures are near 0 °C. The surface brightness temperature is a linear combination of the bare ice brightness temperature and the brightness temperature of the melt ponds covering the ice. Therefore, this constant brightness temperature can be combined with open water brightness temperature, weighted by the fraction of melt ponds forming throughout the ~~summer~~ ~~warm~~ ~~months~~. 20 This approach is simple. We have however not found any other approach that could come closer to reality as the sensitivities are very high near 0 °C.

Another problematic component when surface temperatures increase ~~in spring and summer towards warm conditions~~ is the snow. While the detailed profile of dry snow is not ~~necessarily~~ needed as long as its presence is taken into account for the thermal insulation of the ice and for the refraction of the radiation, ~~wet snow has a much higher influence on microwave emission~~. ~~As the influence of wet snow on microwave radiation is much larger. Because~~ in the case of melting snow, ~~very~~ precise information about the ~~snow structure, e.g. wetness distribution, correlation length, and form of snow grains, are~~ ~~wetness distribution in the snow is~~ needed, we cannot come close to simulate realistic brightness temperatures from GCM output. In our experiments we have ignored this effect by setting the snow wetness to zero at all times. However, for an all-year-round realistic simulation of brightness temperatures, we suggest to exclude data containing melting snow from the brightness temperature 25 simulation. ~~As periods of wet snow due to melting or advection of warm air, are typically locally limited in time, we argue that our suggestions enable the simulation of brightness temperature simulations over a large amount of the year.~~

5.3 Outlook

The evaluation framework in this study can be used to explore simulated brightness temperatures at higher frequencies, nearer to the most used operational frequencies. However, snow is a limiting factor in this case. While the radiative effect of ~~the a dry~~ snow cover is small at 6.9 GHz, its impact increases with increasing frequency. It becomes therefore more important to know

5 the snow structure, e.g. snow density, snow temperature, and snow scatterer structure. This information is lacking in GCMs. As the snow structure is more dynamic and changes faster than the ice structure, parametrization for the snow structure do not exist yet to our knowledge. It would be of high interest to explore the evolution of snow on sea ice in more details and perform sensitivity studies to identify possible simplifications. These could eventually lead to realistic brightness temperatures simulated based on GCM output at higher frequencies than 6.9 GHz.

10 Finally, our analysis focuses on the simulation of brightness temperatures based on output from a GCM which simulates sea ice with a very simple sea-ice model. The use of output from GCMs that simulate sea ice with more complex sea-ice models might yield lower uncertainty in the brightness temperature simulation. However, although these models compute many physical properties inside the ice, they do not necessarily store them for each time step. Using the more complex properties of these models would therefore require one to build the emission model into the model code, instead of applying an "external" 15 operator to already produced model output.

6 Conclusions

With the help of a one-dimensional thermodynamic sea-ice model and a one-dimensional emission model, we investigated if realistic sea-ice brightness temperatures can be simulated based on GCM output at a frequency of 6.9 GHz with vertical polarization. We conclude that it is possible to simulate realistic sea-ice brightness temperatures ~~depending on if~~ the time of 20 year and ~~on the boundary conditions~~.

boundary conditions are taken into account. We propose the following structure for an observational operator for sea ice at 6.9 GHz, vertical polarization:

Periods of cold conditions

25 – **Periods of cold conditions:** Use the temperature profile provided by the GCM if existing. Otherwise, use the simulated snow surface ~~temperatur to infer the ice surface temperature and interpolate a temperature and oceant temperature at the bottom of the ice to infer a two-step~~ linear temperature profile through the ~~iee from there~~ ~~snow and ice~~.

– Use the salinity profile provided by the GCM if existing. Otherwise, interpolate the salinity profile as a function of depth, following the functions given by Griewank and Notz (2015).

30 – Apply an emission model, e.g. MEMLS, to these profiles, combined with information about correlation length, sea-ice type, etc.

- Use sea-ice concentration and atmospheric properties provided by the GCM.
- Apply a simple ocean emission model and atmospheric radiative transfer model ~~, e.g. Wentz and Meissner (2000)~~, to account for the ~~effect influence~~ of open water when the sea-ice concentration is below 100% and for the ~~effect influence~~ of the atmosphere ~~on the brightness temperature measurements by satellites from space~~.

5 Periods of bare ice near 0 °C

- ~~Periods of bare ice near 0 °C~~: Use a constant brightness temperature for the ice surfaces. ~~? derive a summer~~ ~~Burgard et al. (2020) derive a warm conditions~~ sea-ice surface brightness temperature of 266.78 K from observational estimates. This represents a brightness temperature at the top of the atmosphere of 262.29 K corrected by the mean atmospheric effect of 4.49 K in their simulations. ~~Weight this constant brightness temperature with the~~
- Use sea-ice concentration, melt pond fraction, and atmospheric properties provided by the GCM.
- Apply a simple ocean emission model and atmospheric radiative transfer model ~~, e.g. Wentz and Meissner (2000)~~, to account for the ~~effect influence~~ of open water when the sea-ice concentration is below 100% ~~or when melt ponds are present on the ice~~ and for the ~~effect influence~~ of the atmosphere ~~on the brightness temperature measurements by satellites from space~~. If not existing yet, include a routine accounting for the effect of melt ponds additionally to the effect of open ocean surfaces in the surface emission model.

Periods of melting snow

- ~~Periods of melting snow~~: ~~Identify periods and locations of reduction in snow thickness at temperatures near 0 °C in the GCM output.~~
- Ignore these points in the analysis. The GCM output does not provide enough information about the snow properties and wet snow strongly affects the brightness temperature.

The observational operator structure we present here allows us to simulate brightness temperatures from two-dimensional output by a GCM that can be compared with brightness temperatures measured by satellites. This opens new possibilities and perspectives for model-to-observation comparison in the Arctic Ocean.

Code and data availability. Primary data and scripts used in this study are archived by the Max Planck Institute for Meteorology and can be

25 obtained by contacting publications@mpimet.mpg.de.

Appendix A: Retrieving sea-ice properties from temperature and salinity

The following formulas were used to compute the ice density ρ_i and brine volume fraction Φ_l profiles from the ice temperature T and salinity S profiles (Notz, 2005):

$$\rho_0 = 916.18 - 0.1403T \quad (A1)$$

5 where ρ_0 is the density of pure ice (Pounder, 1965).

$$S_b = \frac{-17.6T - 0.389T^2 - 0.00362T^3}{\begin{cases} 508.18 + 14.535T + 0.2018T^2 & \text{if } T \in [-43.2^\circ\text{C}, -36.8^\circ\text{C}] - \text{Eq. (39) in Vant et al. (1978)} \\ 242.94 + 1.5299T + 0.04529T^2 & \text{if } T \in [-36.8^\circ\text{C}, -22.9^\circ\text{C}] - \text{Eq. (39) in Vant et al. (1978)} \\ -1.20 - 21.8T - 0.919T^2 & \text{if } T \in [-22.9^\circ\text{C}, -8.0^\circ\text{C}] - \text{Eq. (3.4) in Notz (2005)} \\ 1/(0.001 - (0.05411/T)) & \text{if } T \in [-8.0^\circ\text{C}, 0^\circ\text{C}] - \text{Eq. (3.5) in Notz (2005)} \\ 0 & \text{if } T = 0 \end{cases}} \quad (A2)$$

where S_b is the brine salinity.

$$\rho_w = 1000.3 + 0.78237S_b + 2.8008 \cdot 10^{-4}S_b^2 \quad (A3)$$

where ρ_w is the density of seawater (at 0°C (Eq. (3.8) in Notz, 2005)).

$$10 \quad \Phi_l = \frac{S/S_b}{\begin{cases} S/S_b & \text{if } S_b > 0 - \text{Eq. (1.5) in Notz (2005)} \\ 1 & \text{if } S_b = 0 \end{cases}} \quad (A4)$$

$$\rho_i = \Phi_l \cdot \rho_w + (1 - \Phi_l) \cdot \rho_0 \quad (A5)$$

15 The following formula was used to infer the ice surface temperature $T_{\text{ice,surf}}$ from the snow surface temperature $T_{\text{snow,surf}}$:

$$T_{\text{ice,surf}} = \frac{T_{\text{snow,surf}} \cdot \frac{k_s}{h_s} + T_{\text{bottom}} \cdot \frac{k_i}{h_i}}{\frac{k_s}{h_s} + \frac{k_i}{h_i}} \quad (A6)$$

with k_s the thermal conductivity of snow (= 0.31 $\text{W/Km} \text{WK}^{-1} \text{m}^{-1}$), k_i the thermal conductivity of ice (= 2.17 $\text{W/Km} \text{WK}^{-1} \text{m}^{-1}$), h_s the snow thickness, h_i the ice thickness, T_{bottom} the temperature at the bottom of the ice, set to -1.8 °C.

Table B1. Formulas describing salinity as a function of depth, [from Griewank and Notz \(2015\)](#), as shown in the full lines in Fig. 5.

Ice type	Salinity parametrization as a function of depth z	Constants needed
First-year ice S_{fy}	$\frac{z}{a+bz} + c$	$a = 1.0964, b = -1.0552,$ $c = 4.41272$
Multiyear ice S_{my}	$\frac{z}{a} + \left(\frac{z}{b}\right)^{1/c}$	$a = 0.17083, b = 0.92762,$ $c = 0.024516$
Transition first-year to multiyear ice	$(1 - t) * S_{\text{my}}(z) + t * S_{\text{fy}}(z)$	$t=0$ at start of melt season and $t=1$ at start of freezing season

Appendix B: Salinity parametrization as a function of depth

Author contributions. C.B. carried out all analyses and wrote the manuscript. D.N. and L.T.P. developed the original idea. All authors contributed to discussions.

Competing interests. No competing interests are present.

5 *Acknowledgements.* We thank Stefan Kern for constructive comments and discussions. [We also thank Mohammed Shokr and an anonymous reviewer for the detailed and insightful comments](#). This work was funded by the project "ESA CCI Sea Ice Phase 2".

References

Bailey, D., DuVivier, A., Holland, M., Hunke, E., Lipscomb, B., Briegleb, B., Bitz, C., and Schramm, J.: CESM CICE5 Users Guide, Tech. rep., 2018.

Barber, D., Fung, A., Grenfell, T., Nghiem, S., Onstott, R., Lytle, V., Perovich, D., and Gow, A.: The role of snow on microwave emission and scattering over first-year sea ice, *IEEE T. Geosci. Remote*, 36, 1750–1763, <https://doi.org/10.1109/36.718643>, 1998.

Bunzel, F., Notz, D., Baehr, J., Müller, W., and Fröhlich, K.: Seasonal climate forecasts significantly affected by observational uncertainty of Arctic sea ice concentration, *Geophys. Res. Lett.*, 43, 852–859, <https://doi.org/10.1002/2015GL066928>, 2016.

Burgard, C., Notz, D., Pedersen, L., and Tonboe, R.: The Arctic Ocean Observation Operator for 6.9 GHz (ARC3O) - Part 2: Development and evaluation, *The Cryosphere Discuss.*, in review, <https://doi.org/10.5194/tc-2019-318>, 2020.

10 Dee, D., Uppala, S., Simmons, A., Berrisford, P., Poli, P., Kobayashi, S., Andrae, U., Balmaseda, M., Balsamo, G., Bauer, P., Bechtold, P., Beljaars, A., van de Berg, L., Bidlot, J., Bormann, N., Delsol, C., Dragani, R., Fuentes, M., Geer, A., Haimberger, L., Healy, S., Hersbach, H., Holm, E., Isaksen, L., Kållberg, P., Köhler, M., Matricardi, M., McNally, A., Monge-Sanz, B., Morcrette, J.-J., Park, B.-K., Peubey, C., de Rosnay, P., Tavolato, C., Thébaut, J.-N., and Vitart, F.: The ERA-Interim reanalysis: configuration and performance of the data assimilation system, *Q. J. Roy. Meteor. Soc.*, 137, 553–597, <https://doi.org/10.1002/qj.828>, 2011.

15 Eyring, V., Cox, P., Flato, G., Gleckler, P., Abramowitz, G., Caldwell, P., Collins, W., Gier, B., Hall, A., Hoffman, F., Hurt, G., Jahn, A., Jones, C., Klein, S., Krasting, J., Kwiatkowski, L., Lorenz, R., Maloney, E., Meehl, G., Pendergrass, A., Pincus, R., Ruane, A., Russell, J., Sanderson, B., Santer, B., Sherwood, S., Simpson, I., Stouffer, R., and Williamson, M.: Taking climate model evaluation to the next level, *Nat. Clim. Change*, <https://doi.org/10.1038/s41558-018-0355-y>, 2019.

Flato, G., Marotzke, J., Abiodun, B., Braconnot, P., Chou, S., Collins, W., Cox, P., Driouech, F., Emori, S., Eyring, V., Forest, C., Gleckler, P., Guilyardi, E., Jakob, C., Kattsov, V., Reason, C., and Rummukainen, M.: Evaluation of Climate Models, book section 9, pp. 741–866, Cambridge University Press, Cambridge, United Kingdom and New York, NY, USA, <https://doi.org/10.1017/CBO9781107415324.020>, 2013.

20 Gabarro, C., Turiel, A., Elosegui, P., Pla-Resina, J., and Portabella, M.: New methodology to estimate Arctic sea ice concentration from SMOS combining brightness temperature differences in a maximum-likelihood estimator, *Cryosphere*, 11, 1987–2002, <https://doi.org/10.5194/tc-11-1987-2017>, 2017.

25 Giorgetta, M., Roeckner, E., Mauritsen, T., Bader, J., Crueger, T., Esch, M., Rast, S., Kornblueh, L., Schmidt, H., Kinne, S., Hohenegger, C., Möbis, B., Krismer, T., Wieners, K., and Stevens, B.: The atmospheric general circulation model ECHAM6: Model description, *Tech. Rep. Reports on Earth System Science*, 135/2013, Max Planck Institute for Meteorology, 2013.

Gregory, J., Stott, P., Cresswell, D., Rayner, N., Gordon, C., and Sexton, D.: Recent and future changes in Arctic sea ice simulated by the 30 HadCM3 AOGCM, *Geophys. Res. Lett.*, 29, 28–1–28–4, <https://doi.org/10.1029/2001GL014575>, 2002.

Grenfell, T., Barber, D., Fung, A., Gow, A., Jezek, K., Knapp, E., Nghiem, S., Onstott, R., Perovich, D., Roesler, C., Swift, C., and Tanis, F.: Evolution of electromagnetic signatures of sea ice from initial formation to the establishment of thick first-year ice, *IEEE T. Geosci. Remote*, 36, 1642–1654, <https://doi.org/10.1109/36.718636>, 1998.

Griewank, P. and Notz, D.: Insights into brine dynamics and sea ice desalination from a 1-D model study of gravity drainage, *J. Geophys. Res-Oceans*, 118, 3370–3386, <https://doi.org/10.1002/jgrc.20247>, 2013.

35 Griewank, P. and Notz, D.: A 1-D modelling study of Arctic sea-ice salinity, *Cryosphere*, 9, 305–329, <https://doi.org/10.5194/tc-9-305-2015>, 2015.

Hallikainen, M.: Microwave radiometry of snow, *Adv. Space Res.*, 9, 267–275, [https://doi.org/10.1016/0273-1177\(89\)90494-8](https://doi.org/10.1016/0273-1177(89)90494-8), 1989.

Hallikainen, M. and Winebrenner, D.: The Physical Basis for Sea Ice Remote Sensing, in: *Microwave Remote Sensing of Sea Ice*, edited by Carsey, F., chap. 4, pp. 29–46, American Geophysical Union, 1992.

Huwald, H., Tremblay, L.-B., and Blatter, H.: Reconciling different observational data sets from Surface Heat Budget of the Arctic Ocean 5 (SHEBA) for model validation purposes, *J. Geophys. Res. Oceans*, 110, <https://doi.org/10.1029/2003JC002221>, c05009, 2005.

Hwang, B., Ehn, J., Barber, D., Galley, R., and Grenfell, T.: Investigations of newly formed sea ice in the Cape Bathurst polynya: 2. Microwave emission, *J. Geophys. Res.-Oceans*, 112, C05 003, <https://doi.org/10.1029/2006JC003703>, 2007.

Ivanova, N., Johannessen, O. M., Pedersen, L. T., and Tonboe, R. T.: Retrieval of Arctic Sea Ice Parameters by Satellite Passive Microwave Sensors: A Comparison of Eleven Sea Ice Concentration Algorithms, *IEEE T. Geosci. Remote*, 52, 7233–7246, 10 <https://doi.org/10.1109/TGRS.2014.2310136>, 2014.

Ivanova, N., Pedersen, L., Kern, S., Heygster, G., Lavergne, T., Sørensen, A., Saldo, R., Dybkjaer, G., Brucker, L., and Shokr, M.: Inter-comparison and evaluation of sea ice algorithms: towards further identification of challenges and optimal approach using passive microwave observations, *Cryosphere*, 9, 1797–1817, <https://doi.org/10.5194/tc-9-1797-2015>, 2015.

JAXA: Global Change Observation Mission: Third Research Announcement, Tech. rep., Earth Observation Research Center, Japan 15 Aerospace Exploration Agency, Japan, 2011.

Jezek, K., Perovich, D., Golden, K., Luther, C., Barber, D., Gogineni, P., Grenfell, T., Jordan, A., Mobley, C., Nghiem, S., and Onstott, R.: A broad spectral, interdisciplinary investigation of the electromagnetic properties of sea ice, *IEEE T. Geosci. Remote*, 36, 1633–1641, <https://doi.org/10.1109/36.718635>, 1998.

Lavergne, T., Macdonald Sørensen, A., Kern, S., Tonboe, R., Notz, D., Aaboe, S., Bell, L., Dybkjær, Eastwood, S., Gabarro, C., Heygster, 20 G., Killie, M., Brandt Kreiner, M., Lavelle, J., Saldo, R., Sandven, S., and Pedersen, L.: Version 2 of the EUMETSAT OSI SAF and ESA CCI sea-ice concentration climate data records, *Cryosphere*, 13, 49–78, <https://doi.org/10.5194/tc-13-49-2019>, 2019.

Lee, S.-M., Sohn, B.-J., and Kim, S.-J.: Differentiating between first-year and multiyear sea ice in the Arctic using microwave-retrieved ice emissivities, *J. Geophys. Res.-Atm*, 122, 5097–5112, <https://doi.org/10.1002/2016JD026275>, 2017.

Lemmettyinen, J., Derksen, C., Rott, H., Macelloni, G., King, J., Schneebeli, M., Wiesmann, A., Leppänen, L., Kontu, A., and Pulliainen, 25 J.: Retrieval of Effective Correlation Length and Snow Water Equivalent from Radar and Passive Microwave Measurements, *Remote Sensing*, 10, 170, <https://doi.org/10.3390/rs10020170>, 2018.

Li, C., Notz, D., Tietsche, S., and Marotzke, J.: The Transient versus the Equilibrium Response of Sea Ice to Global Warming, *J. Climate*, 26, 5624–5636, <https://doi.org/10.1175/JCLI-D-12-00492.1>, 2013.

Light, B., Maykut, G., and Grenfell, T.: Applications of the interaction of microwaves with the natural snow cover, *J. Geophys. Res.-Oceans*, 30 108, <https://doi.org/10.1080/02757258709532086>, 2003.

Mahlstein, I. and Knutti, R.: September Arctic sea ice predicted to disappear near 2°C global warming above present, *J. Geophys. Res.-Atm*, 117, <https://doi.org/10.1029/2011JD016709>, 2012.

Mätzler, C.: Applications of the interaction of microwaves with the natural snow cover, *Remote Sensing Reviews*, 2, 259–387, <https://doi.org/10.1080/02757258709532086>, 1987.

Mätzler, C.: Relation between grain size and correlation length of snow, *J. Glaciol.*, 48, 461–466, <https://doi.org/10.3189/172756502781831287>, 2002.

Nakawo, M. and Sinha, N.: Growth Rate and Salinity Profile of First-Year Sea Ice in the High Arctic, *J. Glaciol.*, 27, 315–330, <https://doi.org/10.3189/S0022143000015409>, 1981.

NASDA: AMSR-E Data Users Handbook, Tech. Rep. NCX-030021, Earth Observation Center, National Space Development Agency of Japan, Japan, 2003.

Niederdrenk, A. and Notz, D.: Arctic sea ice in a 1.5°C warmer world, *Geophys. Res. Lett.*, 45, <https://doi.org/10.1002/2017GL076159>, 2018.

5 Notz, D.: Thermodynamic and Fluid-Dynamical Processes in Sea Ice, Ph.D. thesis, University of Cambridge, 2005.

Notz, D. and Stroeve, J.: Observed Arctic sea-ice loss directly follows anthropogenic CO₂ emission, *Science*, <https://doi.org/10.1126/science.aag2345>, 2016.

Notz, D., Haumann, A., Haak, H., and Marotzke, J.: Arctic sea-ice evolution as modeled by Max Planck Institute for Meteorology's Earth system model, *J. Adv. Model Earth Sy.*, 5, 173–194, <https://doi.org/10.1002/jame.20016>, 2013.

10 Perovich, D., Longacre, J., Barber, D., Maffione, R., Cota, G., Mobley, C., Gow, A., Onstott, R., Grenfell, T., Pegau, W., Landry, M., and Roesler, C.: Field observations of the electromagnetic properties of first-year sea ice, *IEEE T. Geosci. Remote*, 36, 1705–1715, <https://doi.org/10.1109/36.718639>, 1998.

Pounder, E.: *The Physics of Ice*, Elsevier, 1st ed edn., 1965.

15 Proksch, M., Löwe, H., and Schneebeli, M.: Density, specific surface area, and correlation length of snow measured by high-resolution penetrometry, *J. Geophys. Res-Earth*, 120, 346–362, <https://doi.org/10.1002/2014JF003266>, 2015.

Ridley, J., Lowe, J., and Hewitt, H.: How reversible is sea ice loss?, *Cryosphere*, 6, 193–198, <https://doi.org/10.5194/tc-6-193-2012>, 2012.

Shokr, M. and Sinha, N.: Sea ice Properties: Data and Derivations, in: *Sea Ice: Physics and Remote Sensing*, Geophysical Monograph 209, First Edition, edited by Union, A. G., chap. 3, pp. 99–137, John Wiley & Sons, Inc., 2015a.

Shokr, M. and Sinha, N.: Remote Sensing Principles Relevant to Sea Ice, in: *Sea Ice: Physics and Remote Sensing*, Geophysical Monograph 209, First Edition, edited by Union, A. G., chap. 7, pp. 271–335, John Wiley & Sons, Inc., 2015b.

20 Tonboe, R.: The simulated sea ice thermal microwave emission at window and sounding frequencies, *Tellus*, 62A, 333–344, <https://doi.org/10.1111/j.1600-0870.2010.00434.x>, 2010.

Tonboe, R., Andersen, S., Toudal, L., and Heygster, G.: Sea ice emission modelling, in: *Thermal Microwave Radiation - Applications for Remote Sensing*, edited by Mätzler, C., Rosenkranz, P., Battaglia, A., and Wigneron, J., pp. 382–400, IET Electromagnetic Waves Series 52, 2006.

25 Tonboe, R., Dybkjaer, G., and Højer, J.: Simulations of the snow covered sea ice surface temperature and microwave effective temperature, *Tellus*, 63A, 1028–1037, <https://doi.org/10.1111/j.1600-0870.2011.00530.x>, 2011.

Tonboe, R., Eastwood, S., Lavergne, T., Sørensen, A., Rathmann, N., Dybkjær, G., Pedersen, L., Høyer, J., and Kern, S.: The EUMETSAT sea ice concentration climate data record, *Cryosphere*, 10, 2275–2290, <https://doi.org/10.5194/tc-10-2275-2016>, 2016.

30 Ulaby, F., Moore, R., and Fung, A.: Passive microwave sensing of the ocean, in: *Microwave Remote Sensing, Active and Passive Volume III, From Theory to Applications*, chap. 18, pp. 1412–1521, Artech House, Inc., 1986.

Vancoppenolle, M., Fichefet, T., Goosse, H., Bouillon, S., Madec, G., and Morales Maqueda, M.: Simulating the mass balance and salinity of Arctic and Antarctic sea ice. 1. Model description and validation, *Ocean Model.*, 27, 33–53, <https://doi.org/10.1016/j.oceanmod.2008.10.005>, 2009.

35 Vant, M., Ramseier, R., and Makios, V.: The complex-dielectric constant of sea ice at frequencies in the range 0.1–40 GHz, *Journal of Applied Physics*, 49, 1264–1280, <https://doi.org/10.1063/1.325018>, 1978.

Wentz, F. and Meissner, T.: Algorithm theoretical basis document (atbd), version 2, Tech. Rep. AMSR Ocean Algorithm, RSS Tech. Proposal 121599A-1, Remote Sensing Systems, Santa Rosa, CA, 2000.

Wetzel, P., Haak, H., Jungclaus, J., and Maier-Reimer, E.: The Max-Planck-Institute Global Ocean/Sea-Ice Model MPI-OM, Tech. rep., Max Planck Institute for Meteorology, 2012.

Wiesmann, A. and Mätzler, C.: Microwave emission model of layered snowpacks, *Remote Sens. Environ.*, 70, 307–316, 1999.

Willmes, S., Nicolaus, M., and Haas, C.: The microwave emissivity variability of snow covered first-year sea ice from late winter to early summer: a model study, *Cryosphere*, 8, 891–904, <https://doi.org/10.5194/tc-8-891-2014>, 2014.

5 Winebrenner, D., Bredow, J., Fung, A., Drinkwater, M., Nghiem, S., Gow, A., Perovich, D., Grenfell, T., Han, H., Kong, J., Lee, J., Mudaliar, S., Onstott, R., Tsang, L., and West, R.: Microwave Sea Ice Signature Modeling, in: *Microwave Remote Sensing of Sea Ice*, edited by Carsey, F., chap. 8, pp. 137–175, American Geophysical Union, 1992.

Winton, M.: Do Climate Models Underestimate the Sensitivity of Northern Hemisphere Sea Ice Cover?, *J. Climate*, 24, 3924–3934,

10 <https://doi.org/10.1175/2011JCLI4146.1>, 2011.